2014 년 2 월

박사학위논문

Development of Size-, Surface Chemistry– and Shape-controlled PLGA Nanoparticles

조선대학교 대학원

식품의약학과

최 진 석

Development of Size-, Surface Chemistry– and Shape-controlled PLGA Nanoparticles

입자크기, 입자표면수식 및 입자모양이 조절된 PLGA 나노입자의 개발

2014 년 2 월 25 일

조선대학교 대학원

식품의약학과

최 진 석

Development of Size-, Surface Chemistry– and Shape-controlled PLGA Nanoparticles

지도교수 최 후 균

이 논문을 약학박사학위신청 논문으로 제출함.

2013 년 10 월

조선대학교 대학원

식품의약학과

최 진 석

최진석의 박사학위논문을 인준함

위원장 조 선 대 학 교 부교수 최 홍 석 (인)

위 원 조 선 대 학 교 조교수 기 성 환 (인)

위 원 조 선 대 학 교 조교수 신 상 미 (인)

위 원 부 산 대 학 교 조교수 유 진 욱 (인)

위 원 조 선 대 학 교 교수 최 후 균 (인)

2013 년 12 월

조선대학교 대학원

CONTENTS

Chapter 2

Facile size control of PLGA particles in a nano-to-micron scale

Chapter 3

Precisely controlled particle size of paclitaxel-loaded PLGA nano- and microparticles: Influence of particle size on drug delivery

Chapter 4

Fabrication of surface-modifiable nonspherical PLGA particles

List of Tables

Chapter 2

List of Figures

Chapter 2

Chapter 3

Chapter 4

국 문 초 록

입자크기, 입자표면수식 및 입자모양이 조절된 PLGA 나노입자의 개발

최 진 석

지 도 교 수: 최 후 균

식품의약학과

조선대학교 대학원

이 연구의 첫 번째 목적은 크기가 정확하게 제어된 paclitaxel 이 봉입된 PLGA 의 나노와 마이크로 입자의 제조방법을 확립하는 것이다. 두 번째 연구는 PEMA 필름을 이용하여 비 구형입자는 만들어 입자표면을 수식할 수 있도록 만드는 것이다. 다양한 크기의 입자를 에멀젼 프로세스에 의해 만들었다. 다양한 크기의 입자를 가지고 약물 방출, 세포 내 흡수 및 세포 독성을 수행 하였다. 입자의 표면을 수식하기 위해 PVA (하이드록실 사이드 체인) 에서 PEMA (카르복실 사이드 체인) 필름으로 교체하였다. 7 가지 사이즈 (sub-100 nm, 100 nm, 200 nm, 400 nm, 600 nm, 1.0 μm 그리고 2.5 μm) 를 타겟 크기로 설정하고 각 입자를 제조하였다. 좁은 크기 분포를 갖은 7 가지의 크기의 paclitaxel 이 봉입된 PLGA 입자를 만들었다; 70 nm (77.3 ± 13.3 nm), ~100 nm (103.7 ± 15.9 nm), ~200 nm (204.6 ± 26.1 nm), ~400 nm (430.1 ± 71.5 nm), ~600 nm (608.3 ± 116.5 nm), ~1.0 μm (0.98 ± 0.1 μm) and ~2.5 μm (2.45 ± 0.5 μm). 약물방출실험 결과 입자의 크기가 작아질수록 약물방출은 증가했다.

암세포인 KB 에서 paclitaxel 이 봉입된 나노 및 마이크로 입자는 같은 농도에서 독성이 나타났으나 약물자체는 독성이 나타나지 않았다. 세포독성은 입자의 크기에

대한 의존성을 확인했다. 입자의 크기가 작아질수록 높은 독성을 나타냈다. 세포 내 유입실험은 세 가지 크기 (100 nm, 400 nm, 1.0 μm) 의 입자를 가지고 수행되었다. 세포 내 유입 또한 크기와 세포의 종류에 의존적으로 나타났다. 암세포인 KB 에서는 입자의 크기가 작아질수록 세포흡수가 증가 하는 경향을 보여주었으나, 이와는 반대로 대식세포인 Raw 264.7 에서는 입자의 크기가 커질수록 세포흡수가 증가하였다.

비구형의 입자표면에 표면수식이 가능한 카르복실 기의 존재를 확인 하기 위해 FITC-Albumin 의 결합이 가능하도록 입자의 표면을 카보다이미드 방법에 의해 변형한 후 성공적인 합성을 Confocal 현미경을 이용하여 확인하였다.

본 연구결과는 입자의 크기, 표면수식, 입자의 모양이 모두 제어된 paclitaxel 이 봉입된 PLGA 입자는 암세포 표적지향 PLGA 입자 송달 시스템의 발전에 큰 기여를 할 것으로 기대된다.

Chapter 1

Literature Review

:PLGA based on nano- and microparticles for drug delivery

Chapter 1

Literature Review

:PLGA based on nano- and microparticles for drug delivery

1. Introduction

Several problems associated with free drugs such as low solubility, poor stability and unwanted side effects, had led to developing novel drug delivery systems (1). Although various innovative delivery systems have been introduced, there still remains need for further improvement of the issues. Past few decades particle-based delivery systems have been enormously investigated to resolve the problems. The particulate systems have unique advantages over convention formulations, such as protection of unstable drugs, controlled release and targeting ability. Among an array of particulate systems, e.g., polymeric particles, liposomes, micelles, inorganic nanoparticles, PLGA-based micro and nanoparticles are one of the most frequently studied delivery carriers.

Poly(D,L-lactide-co-glycolide), PLGA, is a copolymer composed of lactic acid and glycolic acid. PLGA is one of a few polymers approved by the US FDA for medical purposes due to biodegradability and nontoxicity (2). PLGA in the body degrades by hydrolysis into endogenous monomers, lactic acid and glycolic acid, which subsequently degrade to water and carbon dioxide, resulting in ignorable toxicity (3). By properly choosing molecular weights, the degradation time of PLGA can be modulated from a week to several months, thus enabling drug release in a controlled or sustained manner. Lupron Depot that releases human growth hormone for a month is the first FDA-approved PLGA microparticles implant system. Several other implantable PLGA microparticles have been developed for controlled release of various drugs, some of which obtained the FDA approval. PLGA microparticles have also been widely studied for controlled drug release of oral and pulmonary formulations (4-9). Nano-sized particles prepared with PLGA are an attractive delivery carrier. A majority of PLGA

nanoparticle have been utilized as a tumor-targeting carrier. The small size (less than ~200 nm) and drug loading capacity of PLGA nanoparticles enable targeted delivery to tumors via the enhanced permeability and retention (EPR) effects (10). Surface modification with polyethylene glycol (PEG) make the nanoparticle evade immune responses and reside in the blood circulation for longer time (11), thus enhancing the EPR effects. Non-spherically shaped PLGA particles would also increase the circulation time by avoiding phagocytosis by macrophages (12, 13). Moreover, PLGA nanoparticles are known to enter cells via endocytosis and are able to escape from endosome to release drugs into cytoplasm (14).

As nano- and biotechnology grow rapidly, PLGA particle systems have evolved for more efficient delivery function. The summarized recent drug delivery approaches based on PLGA particle systems in tumor targeting and various administration routes were summarized below.

2. Tumor targeting

Despite better understanding of tumor biology and advancement in diagnostic technologies and treatments, a majority of current cancer therapies still involve aggressive processes including surgery, radiation and chemotherapy, which destroy tumor as well as healthy cells, causing unwanted side effects to patients. It would be therefore desirable to develop effective treatments that have an ability to precisely target and kill the cancer cells while leaving healthy cells unaffected. Efforts have been made to develop nanoparticles that allow chemotherapeutics to accumulate exclusively in cancer cells either passively or actively (15). Nano systems can offer various advantages over free drugs in anticancer drug delivery (16) ; 1) protection of the drug from premature degradation, 2) enhancement of drug deposition into target tumors, 3) control of the PK/PD profile, and 4) improvement of intracellular penetration. Among various polymers and inorganic materials that have been used for tumor-targeting systems, PLGA have long been employed to target tumor cells and delivery antitumor agents in a controlled manner.

In recent years, a number of innovative and novel tumor-targeting approaches using PLGA particles have been developed to enhance tumor targeting ability, thus improving therapeutic

effects.

Active targeting can be achieved by tethering targeting ligands on the particle surface, which recognizes a cell-surface target, followed by uptake of the particles into tumor cells via endocytosis. Traditionally, transferrin and folic acid have been used for PLGA nanoparticles as tumor-targeting ligands (17, 18). Several new targeting ligands have been recently introduced and evaluated.

Antibodies that specifically interact with the receptors can be good candidates for an active tumor-targeting ligand. Fas receptor is a member of the tumor necrosis factor (TNF) super family, which expresses on the plasma membrane of various tumor cells (19, 20). McCarron et al. (21) incorporated camptothecin into PLGA nanoparticles and functionalized the surface with anti-Fas antibody. The anti-Fas-functionalized PLGA nanoparticles were internalized into human colorectal cells more effectively than plain counterparts. IC50 value was also significantly decreases with antibody-PLGA nanoparticles as compared to a camptothecin solution and non-coated nanoparticles, indicating anti-Fas antibody is a good tumor-targeting ligand. Epidermal growth factor receptor (EGFR) was used as a target receptor for targeted PLGA nanoparticles. EGFR is highly expressed on a variety of tumors including breast cancer and ovarian cancer (22). Acharya et al. (23) conjugated anti-EGFR antibody on rapamycin-loaded PLGA nanoparticles. The antibody-coated PLGA nanoparticles showed greater antiproliferation activity by arresting a cell-cycle at G1 phase and more apoptosis as well as necrosis in KB cells in comparison to non-targeted nanoparticles.

Aptamers are oligonucleic acid or peptide molecules that bind to a target molecule with high affinity and selectivity (24). Since aptamers can be produced by chemical synthesis, they are a good alternative to antibodies which requires intensive works and high cost for production. Dhar et al. (25) prepared the aptamers-labeled PLGA nanoparticles containing anticancer drug, cisplatin, for the treatment of prostate cancer. The aptamers was used to target the prostate-specific membrane antigen which is overexpressed in uptake of cisplatin and even higher toxicity as compared to free cisplatin or nanoparticles without aptamers. In another study, paclitaxel-loaded PLGA nanoparticles were surface-functionalized with anti-nucleolin

aptamers (26). The presence of aptamers substantially promoted cellular uptake of the nanoparticles and enhanced apoptotic activities.

Peptides have also been utilized as tumor-targeting ligands. RGD, a tripeptide arginine–glycine–aspartic acid specifically bind to the αvβ3 integrin which are highly expressed only tumor endothelial cells (27). RGD-coated PEGylated PLGA nanoparticles were developed to delivery paclitaxel to tumors (28). In vivo study in mice demonstrated that anti-cancer activity of PLGA nanoparticles are considerably enhanced in the presence of RGD in comparison to non-targeted ones. Luo et al. (29) investigated whether LyP-1, a 9-amino acid cyclic peptide, which was identified by an in vivo phage display technology has a targeting ability to lymphatic tumors. LyP-1-functionalized PLGA-PEG nanoparticles were fourfold more effectively internalized into tumor cells in vitro and eightfold more effectively accumulated in lymphatic metastatic tumors in vivo.

PLGA nanoparticles have been used for delivery of small interfering RNA (siRNA) for targeted gene silencing because they can protect the rapid degradation of siRNA in plasma and cytoplasm by various RNase and facilitate cellular uptake (30). Zhou et al. (31) developed multifunctional PLGA nanoparticles that are suitable for siRNA delivery. The multifunctional nanoparticles, so called octa-functional nanoparticles, were fabricated with PLGA-PLL-PEG-iRGD and loaded with siRNA against PLK1 for modulating tumor growth. The octa-functional nanoparticles showed siRNA stabilization, controlled release of siRNA, endosomal escape, tumor targeting, cell penetration and prolonged knockdown of PLK1, proving the true multifunctional ability. Gene silencing by siRNA was also employed to knockdown the drug efflux transporter to overcome tumor drug resistance. Patil et al. (32) prepared paclitaxel-loaded PLGA nanoparticles along with siRNA against P-glycoprotein (P-gp) and functionalized the nanoparticles with biotin for active targeting. In vitro study showed that cell cytotoxicity was significantly increased when siRNA against P-gp was co-encapsulated with paclitaxel as compared to when only paclitaxel was loaded. In vivo study demonstrated that siRNA efficiently inhibit P-gp expression, resulting in significantly improved inhibition of tumor growth. Although PLGA nanoparticles have potential to delivery siRNA, one should be

aware of the fact that a low loading efficiency of siRNA in PLGA nanoparticles are still a barrier for PLGA nanoparticle-based siRNA delivery systems.

Another strategy to avoid multidrug resistance is the co-encapsulation of P-gp modulators with anticancer drugs. Song et al.(33) loaded vincristine into PLGA nanoparticles along with a P-gp inhibitor, verapamil. Patil et al. (34) fabricated PLGA nanoparticles which encapsulated with paclitaxel and third generation of P-gp inhibitor, tariquidar. Both studies demonstrated that addition of P-gp modulators to anticancer drug-loaded PLGA nanoparticles is able to reverse the multidrug resistance and synergistically enhance cytotoxicity in drug-resistance tumor cells.

3. Pulmonary delivery

Since the lung is an organ that is directly connected from the outside, pulmonary drug delivery is an attractive way for the treatment of local lung diseases such as lung cancer, cystic fibrosis and tuberculosis. The lung has ~300 million alveoli providing extremely high surface area with a well-developed capillary network and low enzymatic activities, which makes efficient absorption of drugs and macromolecules for systemic delivery (35). Lack of targeted deposition and rapid elimination of drugs are, however, barriers for effective pulmonary delivery (36). Particulate systems containing therapeutic agents have been extensively investigated to circumvent the problems for effective treatments of various lung diseases. Due to non-toxicity for lung tissue and lung macrophages (37-39), PLGA micro and nanoparticles have been widely used for pulmonary particulate delivery systems.

Inhalable PLGA particles have been used for the treatment of lung. Susarez et al. (40) developed and evaluated PLGA microparticles loaded with rifampicin. The PLGA particles were intended to target alveolar macrophages to reduce systemic toxicity. Rifampicin-PLGA particles were administered by nebulization and insufflation methods, showing 10-fold-reduced lung bacterial burden as compared to rifampicin alone. Very recently, PLGA nanoparticles systems embedded in a microcarrier, called nano-embedded micro-particles (NEM) have been

developed for lung delivery of antibiotics (41). In this study, lactose was used as an inert microcarrier to ameliorate flow and aerosolization properties and tobramycin, which is a first line drug for cystic fibrosis treatment, was used as an antibiotics. On the surface of PLGA nanoparticles, various helper polymers such as alginate and chitosan were used for optimization of particle properties. The results showed that the dry powder of NEM formulation provided a good flow and deposition to lung, while unique features of PLGA nanoparticles were preserved.

Pulmonary gene delivery is a promising strategy for treating lung diseases. DNA vaccine, which uses DNA encoding tuberculosis antigen to induce immunogenicity, is an attractive strategy for tuberculosis control. For pulmonary DNA delivery, PLGA nanoparticles were fabricated in the presence of a cationic polymer, polyethyleneimine (PEI) (42). The PLGA–PEI nanoparticle showed a cellular uptake by human bronchial epithelial cells, resulting in protein expression. The same nanoparticles also showed effective in vivo proliferation of T cells and interferon-α production by aerosol inhalation in mice whereas intramuscular administration of the same DNA vaccine was not as effective (43). siRNA has also been encapsulated in PLGA nanoparticles for pulmonary delivery. Jensen et al. (44) prepared siRNA-loaded PLGA nanoparticles using a cationic lipid to improve the gene silencing activity. The nanoparticles were then spray dried with a sugar excipient to an inhalable dry microparticle powder, which is similar to NEM approach as mentioned above. The final dry powder containing PLGA-siRNA nanoparticles had good aerodynamic properties while preserving gene silencing activity of siRNA. This study suggested that spray-dried powders composed of PLGA-siRNA nanoparticles have potential for pulmonary siRNA delivery.

The lung is an attractive delivery route of therapeutic proteins, which has a low oral bioavailability due to an enzymatic degradation and a poor absorption. Insulin is the most widely studied protein for pulmonary applications. PLGA particulate systems have been employed to improve therapeutic effects of insulin via lung. The PLGA-insulin PLGA particles were often suspended in an aqueous solution and administered by a nebulizer (45). While the nebulized PLGA-insulin particles prolonged a release profile and protected insulin from an

enzymatic degradation, a severe burst release of insulin was observed. In order to avoid an aqueous formulation and provide a portability and convenience, dry powder systems have been attempted in recent years. Insulin-loaded PLGA microparticles fabricated by using an oil-in-oil method showed a minimized burst release and improved protein stability in vitro (46). The pulmonary absorption of the same PLGA-insulin microparticles was tested in a diabetic rat model (47). As compared to respirable insulin powder and subcutaneous injection of insulin, inhaled PLGA-insulin microparticles had a sustained release profile and a prolonged hypoglycemic activity, indicating of an effectiveness of the dry microparticle system. Large porous particles (LPP), which enables a deep lung deposition due to their good aerodynamic characteristic and avoidance of phagocytic clearance due to their large size (10–20 μm) (48), also have been adapted for pulmonary insulin delivery. However, a use of salts to make porous PLGA particles may harm a stability of insulin (49). Ungaro et al. (50) developed insulin-loaded PLGA LPP using hydroxypropyl-β-cyclodextrin (HPβCD). HPβCD is a good osmotic agent while not affecting insulin integrity. The following in vivo study demonstrated that the PLGA LPP administered by a dry powder inhaler reaches the alveoli region and significantly lowers blood glucose level as compared to the sprayed insulin solution of the same dose (51).

4. Oral delivery

Oral is the most widely used route for drug delivery due to high absorptive surface area in the gastrointestinal track and high patient acceptance. Despite the obvious advantages, poor solubility and low stability by an enzymatic degradation, which result in poor bioavailability, limit the use of many drugs including peptides, proteins and chemotherapeutics. Recently, nanoparticle systems have emerged as an alternative formulation to overcome the problems because they have unique properties such as a protection of drugs, a targeted delivery and a controlled release (52).

One of the most difficult drugs to deliver via the oral route is insulin (53). High hydrophilicity, molecular weight and susceptibility to enzymes make insulin challenging to be

absorbed from the gastrointestinal mucosa. To improve the bioavailability of insulin, PLGA nanoparticles encapsulated with insulin–sodium oleate (SO) complex was developed (54). Since insulin is too hydrophilic to obtain a sufficient loading amount in hydrophobic

PLGA nanoparticles, SO, an anionic surfactant, was used to form a complex system with positively charged insulin, thus increasing hydrophobicity (55). The loading efficiency of insulin was approximately 90 %. In vivo study showed that oral administration of insulin–SO complex-loaded PLGA nanoparticles significantly enhanced bioavailability and reduced the blood glucose level for a prolonged period of time. In another study, dual-functional PLGA nanoparticles were designed to efficiently delivery insulin to the upper region of the small intestine (56). To enhance the penetration of insulin into mucosal layer, cationic polymer, Eudragit® RS, was incorporated with PLGA to prepare the cationic nanoparticles. Then the nanoparticles were placed in the enteric capsule coated with pH-sensitive hydroxypropyl methylcellulose phthalate (HP55) for preventing the premature release in the stomach. The insulin-loaded dual-functional PLGA nanoparticles reduced blood glucose levels in diabetic rat model for an extended period of time. The results of studies presented above imply that protein or peptide drugs including insulin might be orally delivered by PLGA nanoparticles with improved bioavailability.

In addition to insulin, other classes of drugs have been loaded in orally applicable PLGA nanoparticles. Kalaria et al. (57) designed PLGA nanoparticle systems for oral delivery of doxorubicin, which has low oral bioavailability due to the first-pass metabolism, and found that doxorubicin-loaded PLGA nanoparticles markedly increased the oral bioavailability for prolonged time, presumably because of the sustained release of doxorubicin for the nanoparticles. The same research group investigated PLGA nanoparticles for oral delivery of estradiol (58) and amphotericin B (59), and demonstrated that bioavailability of both drugs can be significantly improved by PLGA nanoparticle systems. Curcumin was incorporated in PLGA nanoparticles by a similar method described above and its oral bioavailability was improved by ninefold as compared to an oral curcumin solution with absorption enhancers (60).

5. Ophthalmic delivery

A rapid clearance by lacrimation, tear dilution and tear turnover, leads to a poor bioavailability of eye drops, which is the most commonly used eye formulation. Other ophthalmic formulations such as gels and ointments also have problems of blurred vision, sticking of the eye lid and low patient compliance (61). The impediments of currently used formulations have accelerated research on novel ophthalmic delivery systems composed nanoparticles. Nanoparticles of biodegradable polymers can load various types of therapeutic cargoes, for examples, a poorly water-soluble drugs, proteins and genes and release them in a controlled or sustained manner. Since nanoparticles dispersed in a liquid vehicle have a similar viscosity of conventional eye drops, they would have a good patient acceptance (62).

Mucoadhesive property can be added for higher penetration and prolonged residence time. Recently, PLGA nanoparticles have been studied for efficient delivery of an array of drugs to eyes.

Nonsteroidal anti-inflammatory drugs (NSAIDs) are commonly used drugs to manage ocular inflammations and prevent intra-operative miosis and cystoid macular edema, but their low ocular bioavailability limits the use of the drugs (63). Vega et al. (64) have developed PLGA nanoparticles containing flurbiprofen (FB) to improve the ocular bioavailability which is low with the commercially available eye drop formulations such as Oculflur®. FB was efficiently loaded into PLGA nanoparticles and the nanoparticles released the drug in a controlled manner. The ex vivo study revealed that the corneal permeability of FB was increased by twofold as compared to Oculflur® and by fourfold as compared to FB solution in a pH 7.4 phosphate buffer. Corneal hydration did not change after the application of FB-PLGA nanoparticles, indicating that nanoparticles have no damage to eye tissues. In a following study, it was found that the FB-loaded nanoparticles were physicochemically stable over 75 days and were not irritant to ocular tissues (65). Diclofenac sodium, a poor water-soluble NSAID, was also formulated to nanoparticles using PLGA (66). Diclofenac-loaded PLGA nanoparticles

improved corneal adhesion and did not show any irritancy on cornea, iris and conjunctiva for up to 24 h. A poorly water-soluble anti-bacterial drug, sparfloxacin, was formulated into PLGA nanoparticles. As compared to marketed eye drop formulations, a drug release profile, precorneal residence time and ocular penetration were improved with the PLGA nanoparticle system. The ocular tolerability study using hen's egg chorioallantoic membrane test demonstrated that the PLGA nanoparticles are not irritant (67).

Chang et al. (68), reported on doxycycline-loaded PLGA microparticles for protecting a corneal barrier disruption in dry eye. Instead of nanoparticles, microparticles were chosen for higher loading efficiency and prolonged drug release to overcome inconvenience of daily dose of eye drops. The drug-loaded microparticles in a diameter of 4.6 μm were administered by subconjunctival injection into dry eyes in mice. The results showed that doxycycline-loaded PLGA microparticles had as efficacious as a daily administration of eye drops for 5 days. Ocular delivery of peptide drugs were attempted using PLGA microparticles. Gavini et al. (69), fabricated PLGA microparticles encapsulated with a peptide anti-bacterial drug, vancomycin.

To increase the drug loading efficiency, a novel fabrication method, an emulsification/spray-drying technique, was used instead of a double-emulsion method which is commonly used for protein or peptide encapsulation in PLGA particles. In a rabbit model, vancomycin concentration in the aqueous humor was increased for prolonged time as compared to vancomycin solution. Interestingly, authors added hydroxypropyl cellulose as a suspending agent to PLGA microparticles to improve the residence time and bioavailability; however, the ocular bioavailability did not change, implying that the size of PLGA microparticles can reside in the cul-de-sac and precorneal area, releasing the drug in a controlled manner.

The ocular residence time can be further prolonged with mucoadhesiveness. Jain et al. (70), developed PLGA–chitosan nanoplexes for the purpose. Using a fluorescent dye, the residence time of the nanoplex system and a fluorescent solution were compared. The nanoplexes showed prolonged residence time and higher paracellular and transcellular uptake of the dye as compared to the dye solution, implying that chitosan opens tight junctions and enhances endocytosis processes.

6. Vaginal drug delivery

A majority of vaginal drug delivery systems are intended for the treatment or the prevention of local vaginal abnormalities such as HIV infections, even though well-developed blood vessels under vaginal walls makes the vagina a promising route for a systemic delivery (71).

Particulate systems are suitable to vaginal application due to their thixotropic properties and resistance from pH changes in vaginal mucosa. Nanoparticle delivery systems to the vagina have advantages of a once-a-day vaginal application which can improve patients' compliance.

Since nanoparticles with a diameter of less than 300 nm are able to permeate mucosal membranes which have an average pore size of 340 nm (72), they can be evenly distributed in the vaginal cavity which are composed of the highly folded epithelial surfaces (73). These benefits have accelerated development of novel vaginal delivery systems using micro and nanoparticles.

Vaginal applications of topical microbicides utilizing PLGA nanoparticles have been developed for the prevention and treatment of HIV-1 infection. Ham et al. (74), prepared PLGA nanoparticles containing an analog of naturally occurring chemokine, PSC-RANTES, which modulate a fusion between virus membrane and the cell membrane. By incorporating the drug into PLGA nanoparticles, tissue uptake was increased by five times and tissue permeability was significantly enhanced as compared to the unformulated drug. Degradation of the PSC-RANTES can be also protected in the nanoparticles. A commercialize microbicide, tenofovir, was formulated by PLGA nano systems for a controlled release. Zhang et al. (75) developed novel pH-sensitive tenofovir-loaded nanoparticles composed of PLGA and pH-sensitive polymer, Eudragit-S100. The release rate of tenofovir was controlled by changing a ratio of PLGA and Eudragit-S100. The nanoparticles did not induce any toxicity for 48 h in vaginal cells and Lactobacillus crispatus, suggesting that the novel pH-sensitive nano system is a promising strategy for anti-HIV microbicide delivery.

Blum et al. (76), fabricated topical PLGA nanoparticles loaded with anticancer drug,

camptothecin for the prevention of intravaginal tumor. To test the effectiveness of the nanoparticle system, a vaginal tumor model was established in mice. Camptothecin-loaded PLGA nanoparticles administered by intravaginal lavage completely prevent tumor growth, indicating that topical PLGA nanoparticles are an effective delivery system for the treatment of vaginal tumors.

Since vaginal delivery siRNA using liposomes cannot provide a controlled or sustained release, PLGA nanoparticles were investigated as an alternative to siRNA delivery system.

Woodrow et al. (77) first developed siRNA-loaded PLGA nanoparticles with a high siRNA loading efficiency. The PLGA nanoparticles showed a deep-penetration into vaginal epithelial tissues and induced effective and prolonged gene silencing activity, implying that various siRNA targeting HIV-1 and tumors can be used for vaginal delivery. In a following study, surface-modified PLGA nanoparticles with mucoadhesive avidin and PEG were prepared to find optimal in vivo distribution in a vaginal cavity (78). It was found that PEG-modified PLGA nanoparticles were more effectively penetrate mucus layers and entered vaginal epithelial cells than avidin-modified ones, implying that when designing particulate systems to deliver drug to vaginal cells, surface modification should be rationally considered.

A female sexual arousal disorder is caused by an insufficient vaginal blood flow. Nitric oxide (NO) is a naturally occurring strong vasodilator. However, very short half-life (a few second) of NO impeded the development of NO-delivery systems. Yoo et al. (79) developed a novel NO-releasing PLGA microparticles for virginal applications. DETA NONOate, a NO donor, was used since NO is a gas molecule and cannot be directly incorporated into the particles. It was found that oil-in-oil method protect DETA NONOate during the fabrication process, resulting in a high loading efficiency of the NO donor.

The NO released from the microparticles was found to effectively penetrate a vaginal cell layer and increased the intracellular cGMP level. A following in vivo study in mice demonstrated that the NO-releasing PLGA microparticles are able to significantly increase the vaginal blood flow for the prolonged period of time, suggesting that NO-releasing PLGA microparticles are a promising treatment option for female sexual arousal disorder (71).

7. Conclusion

PLGA micro- and nanoparticles have long been studied for a number of biomedical applications including drug delivery. A good biocompatibility and drug loading capacity as well as modifiable surface properties are key properties that made PLGA particle systems versatile. PLGA particles were used to encapsulate poorly soluble drugs as well as hydrophilic drug such as proteins, peptides, genes and siRNA. Novel fabrication methods such as pore-generating techniques enabled high loading efficiency of various hydrophilic drugs. To improve the performance, different types of materials including chitosan and PEG were mixed or chemically conjugated with PLGA to prepare the particles. Surface of the nanoparticles were functionalized for prolonged circulation time and active targeting. In this literature review, a variety of recently developed PLGA particles systems have been introduced. This information would lead to more effective PLGA-based particulate drug delivery systems.

8. References

1. J.-W. Yoo, D.J. Irvine, D.E. Discher, and S. Mitragotri. Bio-inspired, bioengineered and biomimetic drug delivery carriers. Nature Reviews Drug Discovery. 10:521-535 (2011).
2. R. Di Toro, V. Betti, and S. Spampinato. Biocompatibility and integrin-mediated adhesion of human osteoblasts to poly (DL-lactide-co-glycolide) copolymers. European Journal of Pharmaceutical Sciences. 21:161-169 (2004).
3. X.S. Wuand N. Wang. Synthesis, characterization, biodegradation, and drug delivery application of biodegradable lactic/glycolic acid polymers. Part II: biodegradation. Journal of Biomaterials Science, Polymer Edition. 12:21-34 (2001).
4. M. Aguiar, J. Rodrigues Jr, and A. Silva Cunha. Encapsulation of insulin-cyclodextrin complex in PLGA microspheres: A new approach for prolonged pulmonary insulin delivery. Journal of microencapsulation. 21:553-564 (2004).
5. R. Bhavane, E. Karathanasis, and A.V. Annapragada. Agglomerated vesicle technology: a new class of particles for controlled and modulated pulmonary drug delivery. Journal of Controlled Release. 93:15-28 (2003).
6. G.P. Carino, J.S. Jacob, and E. Mathiowitz. Nanosphere based oral insulin delivery. Journal of Controlled Release. 65:261-269 (2000).
7. A. des Rieux, V. Fievez, M. Garinot, Y.-J. Schneider, and V. Préat. Nanoparticles as potential oral delivery systems of proteins and vaccines: a mechanistic approach. Journal of Controlled Release. 116:1-27 (2006).
8. Y. Dongand S.-S. Feng. Poly (d, l-lactide-co-glycolide)/montmorillonite nanoparticles for oral delivery of anticancer drugs. Biomaterials. 26:6068-6076 (2005).
9. C. Evora, I. Soriano, R.A. Rogers, K.M. Shakesheff, J. Hanes, and R. Langer. Relating the phagocytosis of microparticles by alveolar macrophages to surface chemistry: the effect of 1, 2-dipalmitoylphosphatidylcholine. Journal of Controlled Release. 51:143-152 (1998).
10. S. Acharyaand S.K. Sahoo. PLGA nanoparticles containing various anticancer agents and tumour delivery by EPR effect. Advanced Drug Delivery Reviews. 63:170-183 (2011).

11. R. Gref, Y. Minamitake, M.T. Peracchia, V. Trubetskoy, V. Torchilin, and R. Langer. Biodegradable long-circulating polymeric nanospheres. Science. 263:1600-1603 (1994).
12. J.A. Champion, Y.K. Katare, and S. Mitragotri. Particle shape: a new design parameter for micro-and nanoscale drug delivery carriers. Journal of Controlled Release. 121:3-9 (2007).
13. J.-W. Yooand S. Mitragotri. Polymer particles that switch shape in response to a stimulus. Proceedings of the National Academy of Sciences. 107:11205-11210 (2010).
14. J. Panyam, W.-Z. ZHOU, S. PRABHA, S.K. SAHOO, and V. LABHASETWAR. Rapid endo-lysosomal escape of poly (DL-lactide-co-glycolide) nanoparticles: implications for drug and gene delivery. The FASEB Journal. 16:1217-1226 (2002).
15. I. Brigger, C. Dubernet, and P. Couvreur. Nanoparticles in cancer therapy and diagnosis. Advanced Drug Delivery Reviews (2012).
16. D. Peer, J.M. Karp, S. Hong, O.C. Farokhzad, R. Margalit, and R. Langer. Nanocarriers as an emerging platform for cancer therapy. Nature Nanotechnology. 2:751-760 (2007).
17. Y.B. Patil, U.S. Toti, A. Khdair, L. Ma, and J. Panyam. Single-step surface functionalization of polymeric nanoparticles for targeted drug delivery. Biomaterials. 30:859-866 (2009).
18. S.K. Sahooand V. Labhasetwar. Enhanced antiproliferative activity of transferrin-conjugated paclitaxel-loaded nanoparticles is mediated via sustained intracellular drug retention. Molecular pharmaceutics. 2:373-383 (2005).
19. M. Arruebo, M. Valladares, and Á. González-Fernández. Antibody-conjugated nanoparticles for biomedical applications. Journal of Nanomaterials. 2009:37 (2009).
20. S. Balamurugan, A. Obubuafo, S.A. Soper, and D.A. Spivak. Surface immobilization methods for aptamer diagnostic applications. Analytical and bioanalytical chemistry. 390:1009-1021 (2008).
21. P.A. McCarron, W.M. Marouf, D.J. Quinn, F. Fay, R.E. Burden, S.A. Olwill, and C.J. Scott. Antibody targeting of camptothecin-loaded PLGA nanoparticles to tumor cells. Bioconjugate chemistry. 19:1561-1569 (2008).
22. S.J. Rogers, K.J. Harrington, P. Rhys-Evans, O. Pornchai, and S.A. Eccles. Biological significance of c-erbB family oncogenes in head and neck cancer. Cancer

and Metastasis Reviews. 24:47-69 (2005).

23. S. Acharya, F. Dilnawaz, and S.K. Sahoo. Targeted epidermal growth factor receptor nanoparticle bioconjugates for breast cancer therapy. Biomaterials. 30:5737-5750 (2009).

24. E. Levy-Nissenbaum, A.F. Radovic-Moreno, A.Z. Wang, R. Langer, and O.C. Farokhzad. Nanotechnology and aptamers: applications in drug delivery. Trends in biotechnology. 26:442-449 (2008).

25. S. Dhar, F.X. Gu, R. Langer, O.C. Farokhzad, and S.J. Lippard. Targeted delivery of cisplatin to prostate cancer cells by aptamer functionalized Pt (IV) prodrug-PLGA–PEG nanoparticles. Proceedings of the National Academy of Sciences. 105:17356-17361 (2008).

26. A. Aravind, S.H. Varghese, S. Veeranarayanan, A. Mathew, Y. Nagaoka, S. Iwai, T. Fukuda, T. Hasumura, Y. Yoshida, and T. Maekawa. Aptamer-labeled PLGA nanoparticles for targeting cancer cells. Cancer Nanotechnology. 3:1-12 (2012).

27. P.C. Brooks, R. Clark, and D.A. Cheresh. Requirement of vascular integrin alpha v beta 3 for angiogenesis. Science. 264:569-571 (1994).

28. F. Danhier, B. Vroman, N. Lecouturier, N. Crokart, V. Pourcelle, H. Freichels, C. Jérôme, J. Marchand-Brynaert, O. Feron, and V. Préat. Targeting of tumor endothelium by RGD-grafted PLGA-nanoparticles loaded with paclitaxel. Journal of Controlled Release. 140:166-173 (2009).

29. G. Luo, X. Yu, C. Jin, F. Yang, D. Fu, J. Long, J. Xu, C. Zhan, and W. Lu. LyP-1-conjugated nanoparticles for targeting drug delivery to lymphatic metastatic tumors. International Journal of Pharmaceutics. 385:150-156 (2010).

30. S. Zhang, B. Zhao, H. Jiang, B. Wang, and B. Ma. Cationic lipids and polymers mediated vectors for delivery of siRNA. Journal of Controlled Release. 123:1-10 (2007).

31. J. Zhou, T.R. Patel, M. Fu, J.P. Bertram, and W.M. Saltzman. Octa-functional PLGA nanoparticles for targeted and efficient siRNA delivery to tumors. Biomaterials. 33:583-591 (2012).

32. Y.B. Patil, S.K. Swaminathan, T. Sadhukha, L. Ma, and J. Panyam. The use of nanoparticle-mediated targeted gene silencing and drug delivery to overcome tumor drug resistance. Biomaterials. 31:358-365 (2010).

33. X.R. Song, Z. Cai, Y. Zheng, G. He, F.Y. Cui, D.Q. Gong, S.X. Hou, S.J. Xiong, X.J.

Lei, and Y.Q. Wei. Reversion of multidrug resistance by co-encapsulation of vincristine and verapamil in PLGA nanoparticles. European Journal of Pharmaceutical Sciences. 37:300-305 (2009).

34. Y. Patil, T. Sadhukha, L. Ma, and J. Panyam. Nanoparticle-mediated simultaneous and targeted delivery of paclitaxel and tariquidar overcomes tumor drug resistance. Journal of Controlled Release. 136:21-29 (2009).

35. J.C. Sung, B.L. Pulliam, and D.A. Edwards. Nanoparticles for drug delivery to the lungs. Trends in biotechnology. 25:563-570 (2007).

36. M. Beck-Broichsitter, O.M. Merkel, and T. Kissel. Controlled pulmonary drug and gene delivery using polymeric nano-carriers. Journal of Controlled Release. 161:214-224 (2012).

37. I. Coowanitwong, V. Arya, P. Kulvanich, and G. Hochhaus. Slow release formulations of inhaled rifampin. The AAPS journal. 10:342-348 (2008).

38. D. De Stefano, F. Ungaro, C. Giovino, A. Polimeno, F. Quaglia, and R. Carnuccio. Sustained inhibition of IL-6 and IL-8 expression by decoy ODN to NF-κB delivered through respirable large porous particles in LPS-stimulated cystic fibrosis bronchial cells. The Journal of Gene Medicine. 13:200-208 (2011).

39. K. Hara, H. Tsujimoto, Y. Tsukada, C. Huang, Y. Kawashima, and M. Tsutsumi. Histological examination of PLGA nanospheres for intratracheal drug administration. International Journal of Pharmaceutics. 356:267-273 (2008).

40. S. Suarez, P. O'Hara, M. Kazantseva, C.E. Newcomer, R. Hopfer, D.N. McMurray, and A.J. Hickey. Respirable PLGA microspheres containing rifampicin for the treatment of tuberculosis: screening in an infectious disease model. Pharmaceutical Research. 18:1315-1319 (2001).

41. F. Ungaro, I. d'Angelo, C. Coletta, R. d'Emmanuele di Villa Bianca, R. Sorrentino, B. Perfetto, M.A. Tufano, A. Miro, M.I. La Rotonda, and F. Quaglia. Dry powders

based on PLGA nanoparticles for pulmonary delivery of antibiotics: modulation of encapsulation efficiency, release rate and lung deposition pattern by hydrophilic polymers. Journal of Controlled Release. 157:149-159 (2012).

42. M. Bivas-Benita, S. Romeijn, H.E. Junginger, and G. Borchard. PLGA–PEI nanoparticles for gene delivery to pulmonary epithelium. European Journal of Pharmaceutics and Biopharmaceutics. 58:1-6 (2004).

43. M. Bivas-Benita, M.Y. Lin, S.M. Bal, K.E. van Meijgaarden, K.L. Franken, A.H. Friggen, H.E. Junginger, G. Borchard, M.R. Klein, and T.H. Ottenhoff. Pulmonary delivery of DNA encoding< i> Mycobacterium tuberculosis</i> latency antigen Rv1733c associated to PLGA–PEI nanoparticles enhances T cell responses in a DNA prime/protein boost vaccination regimen in mice. Vaccine. 27:4010-4017 (2009).

44. D.K. Jensen, L.B. Jensen, S. Koocheki, L. Bengtson, D. Cun, H.M. Nielsen, and C. Foged. Design of an inhalable dry powder formulation of DOTAP-modified PLGA nanoparticles loaded with siRNA. Journal of Controlled Release. 157:141-148 (2012).

45. Y. Kawashima, H. Yamamoto, H. Takeuchi, S. Fujioka, and T. Hino. Pulmonary delivery of insulin with nebulized DL-lactide/glycolide copolymer (PLGA) nanospheres to prolong hypoglycemic effect. Journal of Controlled Release. 62:279-287 (1999).

46. J. Emami, H. Hamishehkar, A.R. Najafabadi, K. Gilani, M. Minaiyan, H. Mahdavi, H. Mirzadeh, A. Fakhari, and A. Nokhodchi. Particle size design of PLGA microspheres for potential pulmonary drug delivery using response surface methodology. Journal of microencapsulation. 26:1-8 (2009).

47. H. Hamishehkar, J. Emami, A.R. Najafabadi, K. Gilani, M. Minaiyan, K. Hassanzadeh, H. Mahdavi, M. Koohsoltani, and A. Nokhodchi. Pharmacokinetics and pharmacodynamics of controlled release insulin loaded PLGA microcapsules using dry powder inhaler in diabetic rats. Biopharmaceutics & drug disposition. 31:189-201 (2010).

48. D.A. Edwards, A. Ben-Jebria, and R. Langer. Recent advances in pulmonary drug delivery using large, porous inhaled particles. Journal of Applied Physiology. 85:379-385 (1998).

49. C. Pérezand K. Griebenow. Effect of salts on lysozyme stability at the water–oil

interface and upon encapsulation in poly (lactic-co-glycolic) acid microspheres. Biotechnology and bioengineering. 82:825-832 (2003).

50. F. Ungaro, G. De Rosa, A. Miro, F. Quaglia, and M.I. La Rotonda. Cyclodextrins in the production of large porous particles: development of dry powders for the sustained release of insulin to the lungs. European Journal of Pharmaceutical Sciences. 28:423-432 (2006).
51. F. Ungaro, R. d'Emmanuele di Villa Bianca, C. Giovino, A. Miro, R. Sorrentino, F. Quaglia, and M.I. La Rotonda. Insulin-loaded PLGA/cyclodextrin large porous particles with improved aerosolization properties:< i> In vivo</i> deposition and hypoglycaemic activity after delivery to rat lungs. Journal of Controlled Release. 135:25-34 (2009).
52. L.M. Ensign, R. Cone, and J. Hanes. Oral drug delivery with polymeric nanoparticles: the gastrointestinal mucus barriers. Advanced Drug Delivery Reviews. 64:557-570 (2012).
53. C. Damge, C. Michel, M. Aprahamian, P. Couvreur, and J. Devissaguet. Nanocapsules as carriers for oral peptide delivery. Journal of Controlled Release. 13:233-239 (1990).
54. S. Sun, N. Liang, H. Piao, H. Yamamoto, Y. Kawashima, and F. Cui. Insulin-SO (sodium oleate) complex-loaded PLGA nanoparticles: formulation, characterization and in vivo evaluation. Journal of microencapsulation. 27:471-478 (2010).
55. S. Sun, F. Cui, Y. Kawashima, N. Liang, L. Zhang, K. Shi, and Y. Yu. A novel insulin-sodium oleate complex for oral administration: preparation, characterization and in vivo evaluation. Journal of drug delivery science and technology. 18:239-243 (2008).
56. Z.M. Wu, L. Zhou, X.D. Guo, W. Jiang, L. Ling, Y. Qian, K.Q. Luo, and L.J. Zhang. HP55-coated capsule containing PLGA/RS nanoparticles for oral delivery of insulin. International Journal of Pharmaceutics. 425:1-8 (2012).
57. D. Kalaria, G. Sharma, V. Beniwal, and M.R. Kumar. Design of biodegradable nanoparticles for oral delivery of doxorubicin: in vivo pharmacokinetics and toxicity

studies in rats. Pharmaceutical Research. 26:492-501 (2009).

58. G. Mittal, D. Sahana, V. Bhardwaj, and M. Ravi Kumar. Estradiol loaded PLGA nanoparticles for oral administration: Effect of polymer molecular weight and copolymer composition on release behavior< i> in vitro</i> and< i> in vivo</i>. Journal of Controlled Release. 119:77-85 (2007).

59. J. Italia, M. Yahya, D. Singh, and M.R. Kumar. Biodegradable nanoparticles improve oral bioavailability of amphotericin B and show reduced nephrotoxicity compared to intravenous Fungizone®. Pharmaceutical Research. 26:1324-1331 (2009).

60. J. Shaikh, D. Ankola, V. Beniwal, D. Singh, and M. Kumar. Nanoparticle encapsulation improves oral bioavailability of curcumin by at least 9-fold when compared to curcumin administered with piperine as absorption enhancer. European Journal of Pharmaceutical Sciences. 37:223-230 (2009).

61. Y. Aliand K. Lehmussaari. Industrial perspective in ocular drug delivery. Advanced Drug Delivery Reviews. 58:1258-1268 (2006).

62. R.C. Nagarwal, S. Kant, P. Singh, P. Maiti, and J. Pandit. Polymeric nanoparticulate system: a potential approach for ocular drug delivery. Journal of Controlled Release. 136:2-13 (2009).

63. A.A. Badawi, H.M. El-Laithy, R.K. El Qidra, and H. El Mofty. Chitosan based nanocarriers for indomethacin ocular delivery. Archives of pharmacal research. 31:1040-1049 (2008).

64. E. Vega, F. Gamisans, M. Garcia, A. Chauvet, F. Lacoulonche, and M. Egea. PLGA nanospheres for the ocular delivery of flurbiprofen: drug release and interactions. Journal of pharmaceutical sciences. 97:5306-5317 (2008).

65. J. Araújo, E. Vega, C. Lopes, M. Egea, M. Garcia, and E. Souto. Effect of polymer viscosity on physicochemical properties and ocular tolerance of FB-loaded PLGA nanospheres. Colloids and Surfaces B: Biointerfaces. 72:48-56 (2009).

66. S.M. Agnihotriand P.R. Vavia. Diclofenac-loaded biopolymeric nanosuspensions for ophthalmic application. Nanomedicine: Nanotechnology, Biology and Medicine. 5:90-95 (2009).

67. H. Gupta, M. Aqil, R.K. Khar, A. Ali, A. Bhatnagar, and G. Mittal. Sparfloxacin-loaded PLGA nanoparticles for sustained ocular drug delivery. Nanomedicine: Nanotechnology, Biology and Medicine. 6:324-333 (2010).

68. E. Chang, A.J. McClellan, W.J. Farley, D.-Q. Li, S.C. Pflugfelder, and C.S. De Paiva.

Biodegradable PLGA-based drug delivery systems for modulating ocular surface disease under experimental murine dry eye. Journal of clinical & experimental ophthalmology. 2: (2011).

69. E. Gavini, P. Chetoni, M. Cossu, M.G. Alvarez, M.F. Saettone, and P. Giunchedi. PLGA microspheres for the ocular delivery of a peptide drug, vancomycin using emulsification/spray-drying as the preparation method: in vitro/in vivo studies. European Journal of Pharmaceutics and Biopharmaceutics. 57:207-212 (2004).
70. G.K. Jain, S.A. Pathan, S. Akhter, N. Jayabalan, S. Talegaonkar, R.K. Khar, and F.J. Ahmad. Microscopic and spectroscopic evaluation of novel PLGA–chitosan nanoplexes as an ocular delivery system. Colloids and Surfaces B: Biointerfaces. 82:397-403 (2011).
71. J.-W. Yoo, E.-S. Choe, S.-M. Ahn, and C.H. Lee. Pharmacological activity and protein phosphorylation caused by nitric oxide-releasing microparticles. Biomaterials. 31:552-558 (2010).
72. S.K. Lai, Y.-Y. Wang, K. Hida, R. Cone, and J. Hanes. Nanoparticles reveal that human cervicovaginal mucus is riddled with pores larger than viruses. Proceedings of the National Academy of Sciences. 107:598-603 (2010).
73. K.J. Whaley, J. Hanes, R. Shattock, R.A. Cone, and D.R. Friend. Novel approaches to vaginal delivery and safety of microbicides: biopharmaceuticals, nanoparticles, and vaccines. Antiviral research. 88:S55-S66 (2010).
74. A.S. Ham, M.R. Cost, A.B. Sassi, C.S. Dezzutti, and L.C. Rohan. Targeted delivery of PSC-RANTES for HIV-1 prevention using biodegradable nanoparticles. Pharmaceutical Research. 26:502-511 (2009).
75. T. Zhang, T.F. Sturgis, and B.-B.C. Youan. pH-responsive nanoparticles releasing tenofovir intended for the prevention of HIV transmission. European Journal of Pharmaceutics and Biopharmaceutics. 79:526-536 (2011).
76. J.S. Blum, C.E. Weller, C.J. Booth, I.A. Babar, X. Liang, F.J. Slack, and W.M. Saltzman. Prevention of K-Ras-and Pten-mediated intravaginal tumors by treatment with camptothecin-loaded PLGA nanoparticles. Drug Delivery and Translational Research. 1:383-394 (2011).
77. K. Woodrow, Y. Cu, C. Booth, J. Saucier-Sawyer, M. Wood, and W. Saltzman. Intravaginal gene silencing using biodegradable polymer nanoparticles densely loaded with small-interfering RNA. Nature materials. 8:526-533 (2009).

78. Y. Cu, C.J. Booth, and W.M. Saltzman. < i> In vivo</i> distribution of surface-modified PLGA nanoparticles following intravaginal delivery. Journal of Controlled Release. 156:258-264 (2011).

79. J.W. Yoo, J.S. Lee, and C.H. Lee. Characterization of nitric oxide-releasing microparticles for the mucosal delivery. Journal of Biomedical Materials Research Part A. 92:1233-1243 (2010).

Chapter 2

Facile size control of PLGA particles in a nano-to-micron scale

Chapter 2

Facile size control of PLGA particles in a nano-to-micron scale

1. Introduction

Particulate systems such as polymeric particles, liposomes and micelles, which have their distinctive advantages over conventional formulations in the field of drug delivery and diagnosis have been enormously studied (1, 2). PLGA-based polymeric particles are one of the most extensively studied particle systems among them over last two decades due to their versatility in clinical applications, such as biocompatibility, biodegradability, drug encapsulation, controlled release and modifiable surface chemistry (3). Various parameters in particle design have been investigated to maximize their performance in the body. A type of material, size, shape and surface chemistry are essential parameters that should be considered in designing particulate systems. Optimization of the key particle properties plays a crucial role in an interaction between particles and biological milieu, thus being required for a therapeutic success of the particle systems (4). Since a specific size range should guarantee an efficient delivery of a drug to target diseases, particle size is particularly important. Therefore, in many cases, size is taken first into account in designing particulate systems. The clinically applicable size of PLGA particles ranges from sub-100 nm to a few microns. Nanoscale particles (less than 500 nm) are mostly employed for targeted delivery (i.e. tumor targeted system) to utilize enhanced permeability and retention (EPR) effects or oral formulations for enhanced bioavailability (5). Micron-sized parties are commonly used for pulmonary delivery (0.5 ~ 3 μm) to deliver a drug to the alveoli (6). Larger ones (over 20 μm) can be used or sustained drug release in implant systems such as Lupron® (7). A couple of fabrication technologies have been introduced to produce well-controlled PLGA particles over 3 μm ranges (8). However, the size between sub-100 nm and a few micron, which have been popular for targeted delivery and

lung delivery, have not been well defined until now. For this reason, in most PLGA studies, particle size was rather randomly chosen depending on the fabrication methods which are mostly conventional. Although there have been a few studies that showed a role of particles sizes with well-controlled particle sizes, the particles were made by inorganic materials such as gold and iron oxide (9-11) and their sizes ranged from 10 nm to 80 nm, thus not being applicable to PLGA-based particle systems. There have been efforts to control the particles size by changing polymer concentration, sonication or homogenizer power, PVA concentration, stirring speed; however, those parameter gives only slight modification in size and did not narrow down a size distribution. Subsequently, effects of particles size on drug delivery processes using PLGA-based particles are largely lack. Need for well-established size-controlled fabrication of PLGA particles are emerging. In this study, facile fabrication methods that precisely control particles size in a range between sub 100-nm and a few micron with a high yield and a narrow size distribution were developed.

2. Materials and Methods

2.1. Materials

PLGA copolymers (50:50 DLG 5E, i.v 0.47dL/g) was purchased from Lakeshore Biomaterials (Birmingham, AL, USA). paclitaxel (PTX) was purchased from LC Laboratories (Woburn, MA, USA). PVA (Poly vinyl alcohol); Mw 30,000~70,000, was purchased from Sigma (USA). chloroform, dichloromethane (DCM), acetone and acetonitrile (HPLC grade) were purchased from Burdick & Jackson (Muskegon, MI, USA).

2.2. Preparation of PLGA nano- and microparticles

PLGA nano- and microparticles were prepared by using a variety of different methods: nano-precipitation and solvent evaporation method. The aim of this study is to establish a fabrication method of size-controlled PLGA particles ranging from sub-100 nm to 2.5 μm.

2.2.1. Target size: sub-100 ~ 100 nm

Effects of solvents and power of probe-sonicator: PLGA (50 mg) was dissolved in the three different solvents such as chloroform, acetone and DCM (5 ml respectively). This organic phase was mixed with an aqueous phase 1 % (w/v) of PVA solution (20 ml), the emulsification was done by probe-sonicator (100, 150, 200 and 250 W, 1 min), (KFS-300N ultrasonic processor (Korea)). The resultant emulsion was maintained and allowed to evaporate under mechanical stirring overnight at 500 rpm in the Fume hood. The resultant PLGA particles were centrifuged for 30 min at 20,000 xg for 3 times.

Nano-precipitation method: PLGA (50 mg) was dissolved in 5 ml of acetone. These organic phases were injected into an aqueous 1 % (w/v) of PVA solution (100 ml). The resultant emulsion maintained under mechanical stirring for 18 h at 500 rpm in the Fume hood.

The PLGA particles were centrifuged for 30 min at 20,000 xg for 3 times, the obtained results of 100 nm. 70 nm was obtained simultaneous using injector with homogenizer. Briefly, PLGA (50 mg) was dissolved in 5 ml of acetone. This organic phase was injected into aqueous 1 % (w/v) of PVA solution (100 ml) by injector and the emulsification was done by homogenizer (Ultra-Homogenizer IKA® Ultra-Turrax T-10 (Germany)) with a stirring rate of 20,000 rpm during 9 min in an ice bath. The resultant emulsion maintained under mechanical stirring for 18 h at 500 rpm in the Fume hood. The PLGA particles were centrifuged for 30 min at 20,000 xg for 3 times.

Size separation: PLGA (50 mg) was dissolved in 5 ml of chloroform. This organic phase was mixed with an aqueous 1 % (w/v) of PVA solution (20 ml), the emulsification was done by probe-sonicator (100 W, 1 min). The resultant emulsion maintained under mechanical stirring for 3 h at 500 rpm in the Fume hood. The PLGA particles were centrifuged for 30 min at 20,000 xg for 2 times and centrifuged for 30 min at 6,000 xg, and then supernatant was collected.

2.2.2. Target size: 200 nm

Effects of polymer concentration: PLGA (50 mg) was dissolved in DCM (0.5, 1.0, 1.5 and 2.0 ml respectively). These organic phase were mixed with an aqueous 1 % (w/v) of PVA solution (20 ml), the emulsification was done by probe-sonicator (100 W, 1 min). The resultant emulsion maintained under mechanical stirring for 3 h at 500 rpm in the Fume hood. The PLGA particles were centrifuged for 30 min at 20,000 xg for 3 times.

Effects of PVA concentration: PLGA (50mg) was dissolved in 1.0 ml of DCM. This organic phase was mixed with an aqueous (1, 3 and 7 %) (w/v) of PVA solution (20ml) respectively, the emulsification was done by probe-sonicator (100 W, 1 min). The resultant emulsion maintained under mechanical stirring for 3 h at 500 rpm in the Fume hood. The PLGA particles were centrifuged for 30 min at 20,000 xg for 3 times.

Size separation: PLGA (50 mg) was dissolved in 3 ml of DCM. This organic phase was mixed with an aqueous 3 % (w/v) of PVA solution (9 ml) and then the emulsification was done by probe-sonicator (100 W, 1 min) in an ice bath. The resultant emulsion was poured into an aqueous 1% (w/v) of PVA solution (20 ml) and then maintained under mechanical stirring for 3 h at 500 rpm in the Fume hood. The PLGA particles were centrifuged for 20 min at 1500 xg for 3 times.

2.2.3. Target size: 400 nm

Replacing probe-sonicator with homogenizer: Using a fabrication method of 200 nm; PLGA (50mg) was dissolved in 3 ml of DCM. This organic phase was mixed with 3 % (w/v) of PVA solution (9 ml) and then the emulsification was done by homogenizer (30,000 rpm, 5 min) in an ice bath. The resultant emulsion was poured into an aqueous 1 % (w/v) of PVA solution (20 ml) and then maintained under mechanical stirring for 3 h at 500 rpm in the Fume hood. The PLGA particles were centrifuged for 30 min at 20,000 xg for 3 times.

Size separation: PLGA (50 mg) was dissolved in 3 ml of DCM. This organic phase was mixed with 3 % (w/v) of PVA solution (9 ml) and then the emulsification was done by homogenizer (30,000 rpm, 5 min) in an ice bath. The resultant emulsion was poured into an aqueous 1% (w/v) of PVA solution (20 ml) and then maintained under mechanical stirring for 3 h at 500 rpm in the hood. The PLGA particles were centrifuged for 20 min at 800 xg for 3 times.

2.2.4. Target size: 600 nm

Size separation: PLGA (50 mg) was dissolved in DCM (5 ml and 10 ml respectively). This organic phase was mixed with 30 ml of aqueous 1 % (w/v) of PVA solution, the emulsification was done by homogenizer with a stirring rate of 20,000 rpm during 5 min in an ice bath. The resultant emulsion maintained under mechanical stirring for 3 h at 600 rpm in the Fume hood. The PLGA particles were centrifuged for 20 min at 500 xg for 3 times.

2.2.5. Target size: 1.0 µm

Size separation: PLGA (100 mg) were dissolved in 6 ml of DCM. This organic phase was mixed with 30 ml an aqueous 1 % (w/v) of PVA solution, the emulsification was done by homogenizer with a stirring rate of 30,000 rpm during 5 min in an ice bath. The resultant emulsion maintained under mechanical stirring for 3 h at 500 rpm in the Fume hood. The PLGA particles were centrifuged for 20 min at 250 or 200 xg for 3 times.

2.2.6. Target size: 2.5 µm

Size separation: PLGA (100 mg) was dissolved in 3 ml of DCM. This organic phase was mixed with 30 ml of an aqueous 1 % (w/v) of PVA solution, the emulsification was done by homogenizer with a stirring rate of 20,000 rpm during 5 min in an ice bath. The resultant emulsion maintained under mechanical stirring for 3 h at 600 rpm in the Fume hood. The PLGA particles were centrifuged for 20 min at 100 xg for 3 times.

2.3. Scanning electron microscopy (SEM)

PLGA nano- and microparticles were characterized by using field emission scanning electron microscope (FE-SEM, S4800, Hitachi, Japan). The dispersed PLGA colloid in water was dropped onto a carbon tape and air dried in the Fume hood or desiccator. The carbon tape with PLGA particles were coated with platinum for 2 min under vacuum. The samples were viewed under the FE-SEM at an acceleration voltage of 1~5 kV. The particles size as measured by using ImageJ software (n=100).

2.4. DLS

DLS measurements were performed with a Malvern Zetasizer Nano ZS (Malvern, Herrenberg, Germany) equipped with a 633-nm He-Ne laser and operating at an angle of 173°.

For each sample, 15 runs of 10 s were performed, with three repetitions for all the PLGA nano- and microparticles. The intensity size distribution, the Z-average diameter (Z-ave) and the polydispersity index (PdI) were obtained from the autocorrelation function using the "general purpose mode" for PLGA nano- and microparticles.

3. Results

3.1. Determination of size controlled particles

The PLGA particles with different size ranges were obtained by emulsion process and diverse instruments; from 70 nm to 2.5 μm.

Target size: sub-100 nm and 100 nm: ***Effects of solvents and power of probe-sonicator:*** Three solvents (chloroform, acetone and DCM) were selected and the power of probe-sonicator was used in 4 different levels. The power of probe-sonicator did not affect the size of the particles. On the other hand the difference in the particle size was affected by the solvents. In the case of the use of acetone, the particles ranged from 70 to 90 nm were formed. The resultant particle size using chloroform and DCM showed the nearly similar particle sizes (Figure 1, Table 1).

Nano-precipitation method: The size of 70 and 100 nm were fabricated by using the nano-precipitation method. Acetone is used as the solvent and used injector connected to the instrument. The size of 100 nm was obtained with injector and 70 nm was obtained simultaneous using injector with homogenizer. The results revealed that target size of sub-100 nm and 100 nm showed a narrow distribution particle; 71.5 ± 13.2 nm and 100.0 ± 12.5 nm (Figure 2).

Size separation: The size of 100 nm was obtained by using chloroform (1-1 method), the particles were centrifuged for 30 min at 6,000 xg and the supernatant contained of 80 nm. However, the yield was very low (within 10 %) (Figure 3).

Target size: 200 nm: ***Effects of polymer concentration:*** PLGA (50 mg) was fixed and the volume of DCM was diversified. The size of 100 nm was obtained in PLGA / DCM concentration; 10 mg/ml). Therefore, the volume of DCM was reduced and the concentration

of PLGA was turned up. Consequently, the size increased as the volume of the DCM was decreased. As to (a), there were lots of particles with a large size and the SD value was high. The (b) was near to the target size. (Figure 4, Table 2).

Effects of PVA concentration: PLGA (mg) was fixed and the concentration of PVA was diversified. The PVA concentrations varied from 1 % 3 % and 7 % (w/v) respectively. In the case of the use of 1 % PVA solution, the particles size was closed to 200 nm (198.3 ± 72.2 nm), but there were lots of particles with a large size and the SD value was high. The size was reducing as the PVA concentrations were increased (Figure 5, Table 3).

Size separation: Using 3 % (w/v) of PVA and increasing the volume to 3 ml of DCM, and a size separation by centrifugation for 20 min at 1500 xg for 3 times. The results revealed that the mean of particle size is 216.5 ± 30.9 nm with narrow distribution (Figure 6).

Target size: 400 nm: Based on the manufacturing method of 200 nm, Particle was fabricated by using homogenizer (mean size is 321.4 ± 130.3 nm). The SEM image of (a) showed large particle, and then the particle was used for a size separation by centrifugation. The SEM image of (b) showed 399.6 ± 52.8 nm.

Target size: 600 nm: In the case of the use of PLGA / DCM concentration 10 mg/ml, particle size closed to 650 nm (a) was obtained. By increasing the DCM volume to two times, 600 nm (608.3 ± 116.5 nm) (b) was obtained (Figure 8). A size separation was used for 20 min at 500 xg for 3 times.

Target size: 1.0 µm: DCM volume was decreased in comparison with 600 nm and a size separation by centrifugation was done with 250 xg and 200 xg. When centrifuging with 250 xg, the small particles remained and the average size was under 800 nm. When centrifuging with 200 xg, the average size of the particles of 1.00 ± 0.16 µm were obtained (Figure 9).

Target size: 2.5 µm: The volume of DCM was reduced in comparison with 1.0 µm and the

speed of the homogenizer (rpm) was reduced from 30,000 rpm to 20,000 rpm. A size separation by centrifugation was tested 200 xg and 100 xg. As the result for speed in 200 xg the particles mean size was obtained 2.03 ± 0.57 μm and for 100 xg was obtained 2.46 ± 0.56 μm (Figure 10).

3.2. Fabrication method of size controlled particle in seven sizes

The size of 70 nm and 100 nm was obtained by the nano- precipitation technique. The size of 70 nm was simultaneous used injector with homogenizer and the size of 100 nm was only used injector. Briefly, PLGA (50 mg) was dissolved in 5 ml of acetone. This organic phase was injected into an aqueous 1 % (w/v) of PVA solution (100 ml); the emulsification was done by homogenizer (Ultra-Homogenizer IKA® Ultra-Turrax T-10 (Germany)) with a stirring rate of 20,000 rpm during 9 min in an ice bath. The resulting emulsion maintained under mechanical stirring for 18 h at 500 rpm in the Fume hood.

The size of 200nm and 400 nm was obtained by the solvent evaporation technique. The size of 200 nm was prepared by probe-sonicator (KFS-300N ultrasonic processor (Korea)) and the 400 nm was prepared by homogenizer. Briefly, PLGA (50 mg) was dissolved in 3 ml of DCM. This organic phase was mixed with 3 % (w/v) of PVA solution (9 ml) and then the emulsification was done by probe-sonicator (100 W, 1 min) or homogenizer (30,000 rpm, 5 min) in an ice bath. The resultant emulsion was poured into an aqueous 1% (w/v) of PVA solution (20 ml) and then maintained under mechanical stirring for 3 h at 500 rpm in the Fume hood.

The size of 600 nm was obtained by the solvent evaporation technique. Briefly, 50 mg of PLGA was dissolved in 10ml of DCM. This organic phase was mixed with 30 ml of an aqueous 1 % (w/v) of PVA solution, the emulsification was done by homogenizer with a stirring rate of 30,000 rpm during 5 min in an ice bath. The resultant emulsion maintained under mechanical stirring for 4 h at 500 rpm in the Fume hood.

The size of 1.0 µm was obtained by the solvent evaporation technique. Briefly, PLGA (100 mg) was dissolved in 6 ml of DCM. This organic phase was mixed with an aqueous 1 % (w/v) of PVA solution (30 ml), the emulsification was done by homogenizer with a stirring rate of 30,000 rpm during 5 min in an ice bath. The resultant emulsion maintained under mechanical stirring for 3 h at 500 rpm in the Fume hood.

The size of 2.5 µm was obtained by the solvent evaporation technique. Briefly, PLGA (100 mg) was dissolved in 3 ml of DCM This organic phase was mixed with 30 ml of an aqueous 1 % (w/v) of PVA solution, the emulsification was done by homogenizer with a stirring rate of 20,000 rpm during 5 min in an ice bath. The resultant emulsion maintained under mechanical stirring for 3 h at 600 rpm in the Fume hood.

The nanoparticles with size of 70 and 100 nm were centrifuged for 1 h at 20,000 xg (Lab gene 1736R, Korea) and the particles were washed with distilled water, re-suspended and centrifuged three times to remove the residual PVA and then stored in refrigerator. The separation of other sizes was done by a variety of centrifugation forces (Table 4). The mean size of controlled size of PLGA nano- and microparticles which have been fabricated for 70 nm is (71.5 ± 13.2 nm), ~100 nm is (100.0 ± 12.5 nm), ~200 nm is (216.5 ± 30.9 nm) ~ 400 nm is (399.6 ± 52.8 nm), ~600 nm is (608.3 ± 116.5 nm), ~1.0 µm is (1.00 ± 0.16 µm) and ~2.5 µm is (2.46 ± 0.56 µm) by SEM (Figure 11) and DLS data can be seen in table 5. For all of the targeted size from 70 nm to 600 nm, the size from DLS is bigger than SEM. In addition, as the particle size increases, size difference in between SEM and DLS data also increases and almost it became double. Therefore in this case, particle size data from DLS is not more reliable.

4. Discussion

The aim of this study was to prepare PLGA particles in seven different size ranges from 70 nm to 2.5 µm (70 nm, 100 nm, 200 nm, 400 nm, 600 nm, 1.0 µm and 2.5 µm). The range of different size of PLGA particles were obtained by using solvent evaporation or nano-precipitation method, 70 and 100 nm size particles were obtained by nano-precipitation method and 200 nm ~ 2.5 µm size particles were obtained by solvent evaporation method with probe-sonicator or homogenizer (Figure12). The reproducibility of the particles was over 90 %.

It is considerably difficult to fabricate the sub-100 size particles. In the literature, sub-100 nm size particles were obtained by solvent evaporation method using a probe-sonicator (12, 13). But the particles size was unclear. To fabricate small particles, by increasing the applied energy (instrument power), several parameters were used such as increasing surfactant concentration in an aqueous phase, decreasing polymer concentration, and as well using a mixed instrument (such as injector and homogenizer).

To fabricate sub-100 nm size particles, solvent evaporation and nano-precipitation methods were used. The targeted sub-100 nm size particles were fabricated by using three different solvents (acetone, DCM and chloroform respectively) with probe-sonicator. The 70 nm size particles were obtained with acetone as solvents. When paclitaxel-loaded PLGA particles (70 nm) were fabricated with acetone as solvents by probe-sonicator, the drug was precipitated.

Using chloroform as solvent and a size separation by centrifugation, 80 nm size particles were obtained. But the percentage of the yields was very low, within 10 %.

The size of 100 nm was obtained by using nano-precipitation method with injector. The size of 70 nm was obtained by simultaneously using injector with homogenizer. The PVA concentration and DCM volume were changed variously in order to obtain the size of 200 nm.

By using 3 % (w/v) of PVA and a size separation by centrifugation, and also increasing the volume of the DCM, it revealed that the size of 200 nm was obtained with narrow distribution.

Then by using these fabrication parameters of 200 nm, the 400 nm size particles with narrow

size distribution were obtained by using homogenizer. The 600 nm and 1.0 μm size particles were obtained by changing volume of the solvent and a size separation by centrifugation. The 2.5 μm size particles were obtained by increasing the PLGA concentration and reducing the speed of homogenizer. In this way, the several parameters were changed in order to control the size of the particles.

5. Conclusion

Precise control of particle size ranged from sub-100 nm to a few micrometers was successfully established. The mean size of 70 nm is (71.5 ± 13.2 nm), ~100 nm is (100.0 ± 12.5 nm), ~200 nm is (216.5 ± 30.9 nm) ~400 nm is (399.6 ± 52.8 nm), ~600 nm is (608.3 ± 116.5 nm), ~1.0 μm is (1.00 ± 0.16 μm) and ~2.5 μm is (2.46 ± 0.56 μm) were achieved by using a combination of various methods. The fabrication methods developed in this study would have various applications in the biomedical fields including drug delivery and imaging for diagnosis.

6. References

1. J.-W. Yoo, N. Doshi, and S. Mitragotri. Adaptive micro and nanoparticles: temporal control over carrier properties to facilitate drug delivery. Advanced Drug Delivery Reviews. 63:1247-1256 (2011).
2. J.-W. Yoo, D.J. Irvine, D.E. Discher, and S. Mitragotri. Bio-inspired, bioengineered and biomimetic drug delivery carriers. Nature Reviews Drug Discovery. 10:521-535 (2011).
3. J.-S. Choi, K. Seo, and J.-W. Yoo. Recent advances in PLGA particulate systems for drug delivery. Journal of Pharmaceutical Investigation. 42:155-163 (2012).
4. M.M. Yallapu, B.K. Gupta, M. Jaggi, and S.C. Chauhan. Fabrication of curcumin encapsulated PLGA nanoparticles for improved therapeutic effects in metastatic cancer cells. Journal of colloid and interface science. 351:19-29 (2010).
5. S. Acharyaand S.K. Sahoo. PLGA nanoparticles containing various anticancer agents and tumour delivery by EPR effect. Advanced Drug Delivery Reviews. 63:170-183 (2011).
6. R. Sharma, D. Saxena, A.K. Dwivedi, and A. Misra. Inhalable microparticles containing drug combinations to target alveolar macrophages for treatment of pulmonary tuberculosis. Pharmaceutical Research. 18:1405-1410 (2001).
7. R.C. Mundargi, V.R. Babu, V. Rangaswamy, P. Patel, and T.M. Aminabhavi. Nano/micro technologies for delivering macromolecular therapeutics using poly (d, l-lactide-< i> co</i>-glycolide) and its derivatives. Journal of Controlled Release. 125:193-209 (2008).
8. J. Xieand C.-H. Wang. Electrospun micro-and nanofibers for sustained delivery of paclitaxel to treat C6 glioma in vitro. Pharmaceutical Research. 23:1817-1826 (2006).
9. B.D. Chithrani, A.A. Ghazani, and W.C. Chan. Determining the size and shape dependence of gold nanoparticle uptake into mammalian cells. Nano letters. 6:662-668 (2006).
10. T.K. Sau, A. Pal, N. Jana, Z. Wang, and T. Pal. Size controlled synthesis of gold nanoparticles using photochemically prepared seed particles. Journal of Nanoparticle Research. 3:257-261 (2001).
11. J. Huang, L. Bu, J. Xie, K. Chen, Z. Cheng, X. Li, and X. Chen. Effects of

nanoparticle size on cellular uptake and liver MRI with polyvinylpyrrolidone-coated iron oxide nanoparticles. ACS nano. 4:7151-7160 (2010).

12. R. Yanga, X. Hana, K. Shia, G. Chenga, C.-K. Shimb, and F. Cuia. Cationic formulation of paclitaxel-loaded poly D, L-lactic-co-glycolic acid (PLGA) nanoparticles using an emulsion-solvent diffusion method. Asian J Pharmaceut Sci 2009; 4: 89. 95: (2009).

13. J.S. Park, H.N. Yang, S.Y. Jeon, D.G. Woo, M.S. Kim, and K.-H. Park. The use of anti-COX2 siRNA coated onto PLGA nanoparticles loading dexamethasone in the treatment of rheumatoid arthritis. Biomaterials (2012).

Table 1. Effects of the power and solvent on particle size

Power \ Solvent	chloroform	acetone	dichloromethane
100 W	112.4 ± 18.5 nm	70.5 ± 12.5 nm	108.0 ± 30.9 nm
150 W	102.7 ± 13.5 nm	87.8 ± 15.5 nm	97.6 ± 28.3 nm
200 W	123.4 ± 34.5 nm	93.9 ± 25.1 nm	110.1 ± 27.0 nm
250 W	113.1 ± 20.1 nm	88.7 ± 20.1 nm	115.7 ± 17.3 nm

Table 2. Effect of DCM volume on particle size

Type	DCM Volume	SEM (size ± SD)
(a)	0.5 ml (1.0 %)	235.4 ± 93.4 nm
(b)	1.0 ml (2.0 %)	181.4 ± 73.8 nm
(c)	1.5 ml (3.0 %)	167.4 ± 44.3 nm
(d)	2.0 ml (4.0 %)	156.6 ± 40.9 nm

Table 3. Effect of PVA concentration on particle size

Type	**(a)**	**(b)**	**(c)**
PVA conc.	1 %	3 %	7 %
SEM	198.3 ± 72.2 nm	131.8 ± 25.6	124.8 ± 25.7

Table 4. Condition of a size separation by centrifugation

Target Size	**Centrifuge force (Time)**	**Results**	
		After centrifuge	
200 nm	1,500 xg (20min)	Supernatant : 141.0 ± 20.6 nm	Particles : 216.5 ± 30.9 nm
400 nm	800 xg (20min)	Supernatant : 100~300 nm	Particles : 399.6 ± 52.8 nm
600 nm	500 xg (20min)	Supernatant : 150~400 nm	Particles : 608.3 ± 116.5nm
1.0 μm	200 xg (20min)	Supernatant : 300~800 nm	Particles : 1.00 ± 0.16 μm
2.5 μm	100 xg (20min)	Supernatant : 0.8~1.8 μm	Particles : 2.45 ± 0.56 μm

Table 5. Comparison of the size using DLS and SEM

Target size	**70 nm**	**100 nm**	**200 nm**	**400 nm**	**600 nm**	**1.0 µm**	**2.5 µm**
SEM	71.5 ± 13.2 nm	100.0 ± 12.5 nm	216.5 ± 30.9 nm	399.6 ± 52.8 nm	608.3 ± 116.5nm	1.00 ± 0.16 µm	2.45 ± 0.56 µm
DLS	173.4 nm PDI: 0.072	190.8 nm PDI: 0.035	370.2 nm PDI: 0.032	754.2 nm PDI: 0.032	1091.3 nm PDI: 0.311	n/a	n/a

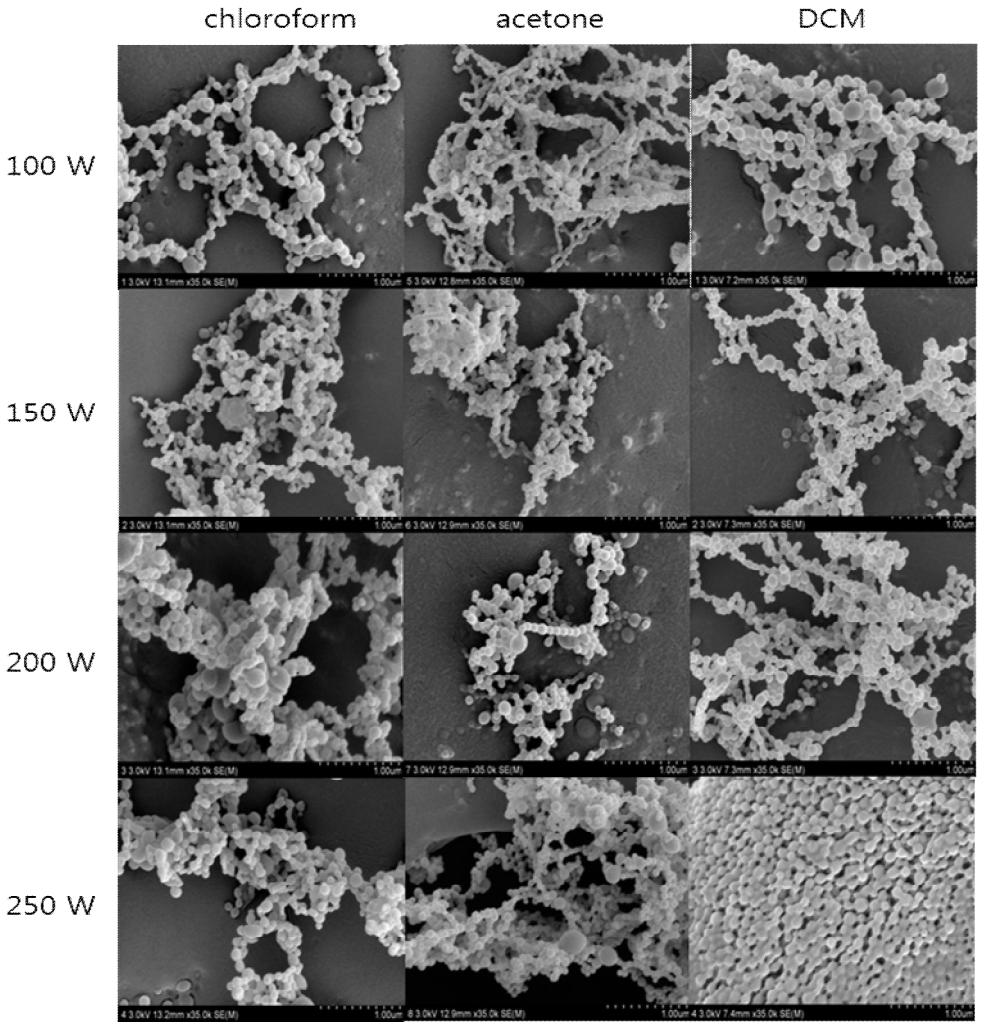

Figure 1. SEM images of the PLGA nanoparticles. The magnification is 35 k.

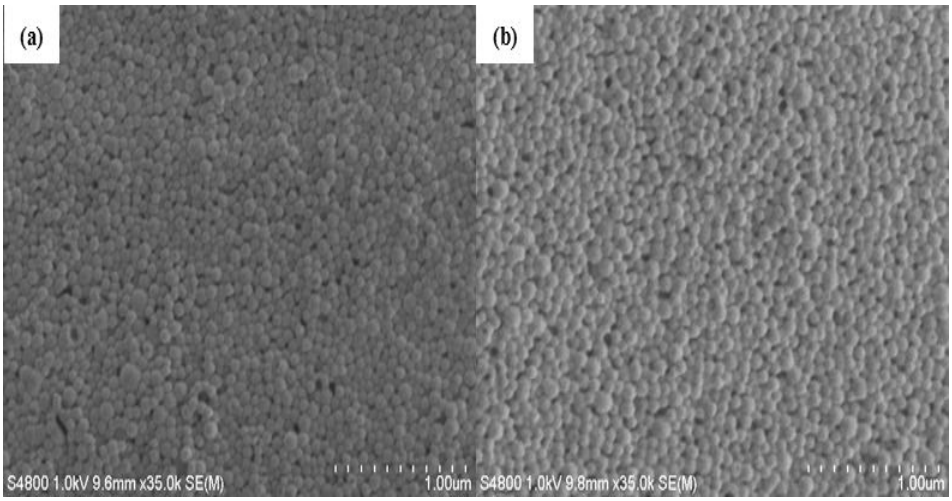

Figure 2. SEM images of targeted size: 70 and 100 nm. The magnification is 35 k, mean size for (a) is 71.5 ± 13.2 nm and (b) is 100.0 ± 12.5 nm.

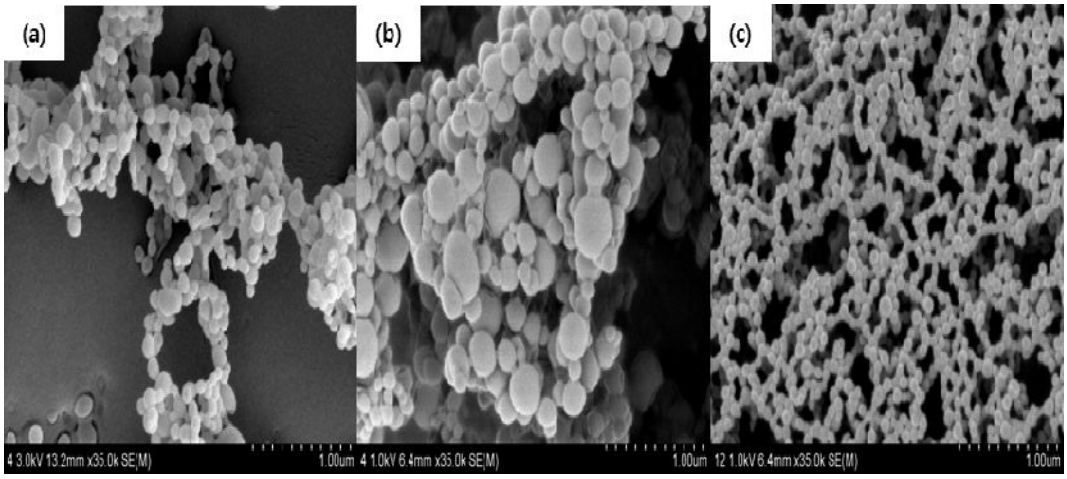

Figure 3. SEM images of targeted size: sub-100 nm. The magnification is 35 k, mean size for (a) is 113.1 ± 20.1 nm, (b) is 164.8 ± 66.0 nm and (c) is 81.6 ± 17.6 nm.

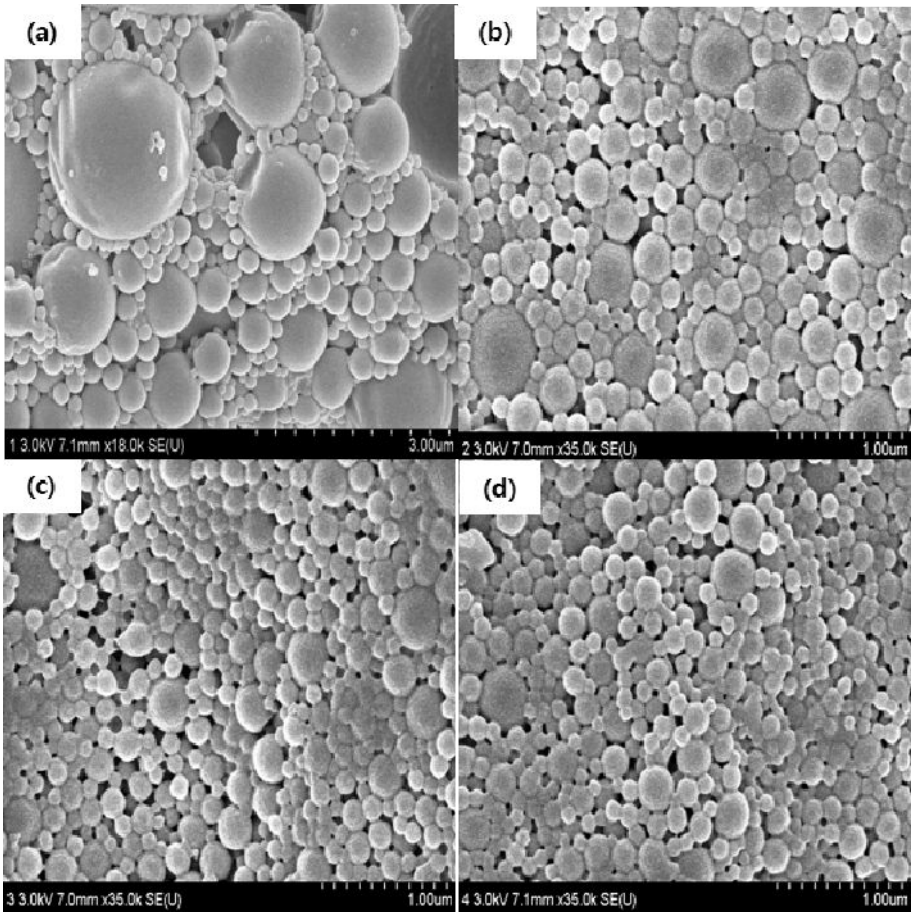

Figure 4. SEM images of the particles obtained by using different DCM volume. The magnification is 35 k.

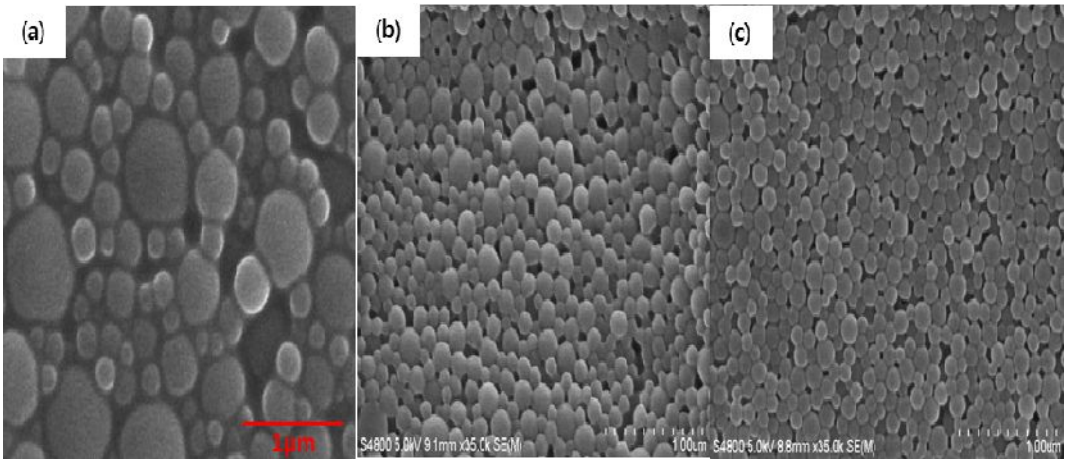

Figure 5. SEM images of the targeted size: 200 nm. The magnification is 35 k, mean size for (a) is 198.3 ± 72.2 nm, (b) is 131.8 ± 25.6 nm and (c) is 124.8 ± 25.7 nm.

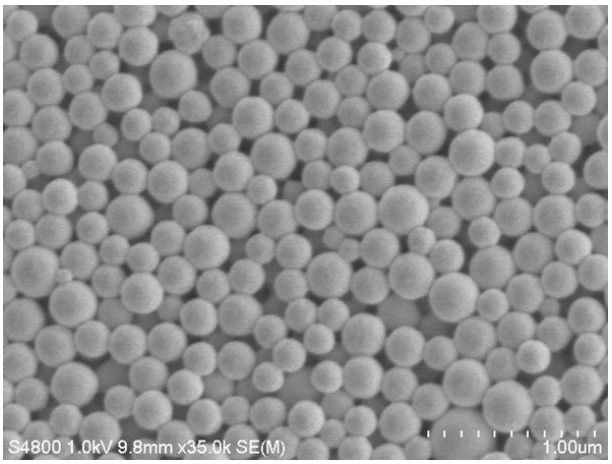

Figure 6. SEM images of the targeted size: 200 nm. The magnification is 35 k, mean size is 216.5 ± 30.9 nm.

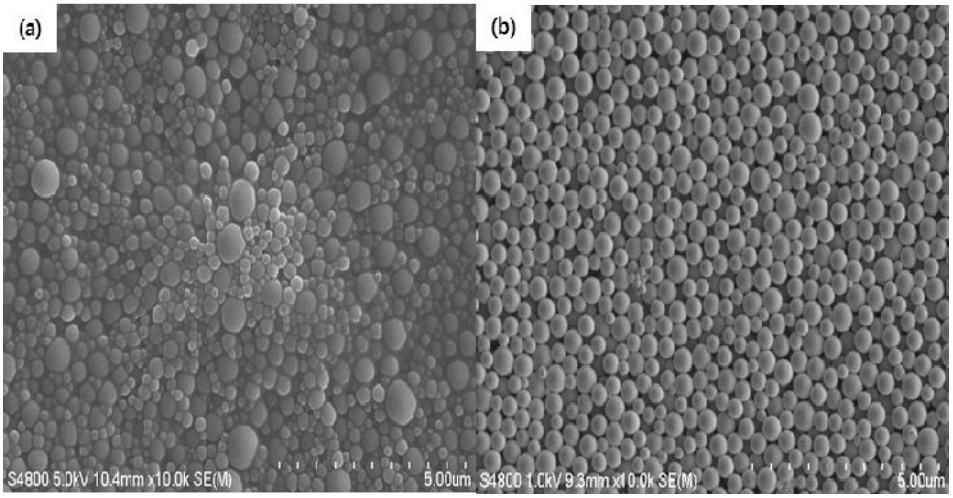

Figure 7. SEM images of the targeted size: 400 nm. The magnification is 10 k, mean size for (a) is 321.4 ± 130.3 nm and (b) is 399.6 ± 52.8 nm.

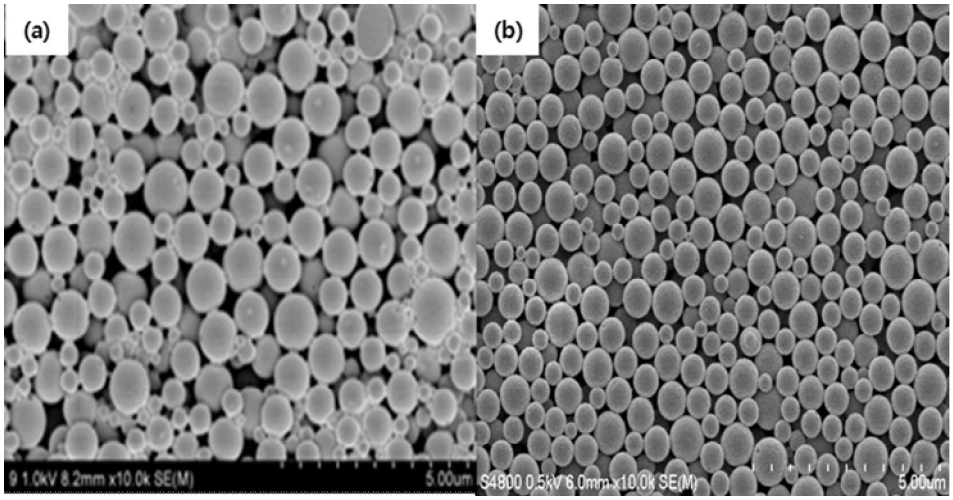

Figure 8. SEM images of the targeted size: 600 nm. The magnification is 10 k, mean size for (a) is 659.0 ± 119.6 nm, and (b) is 608.3 ± 116.5 nm.

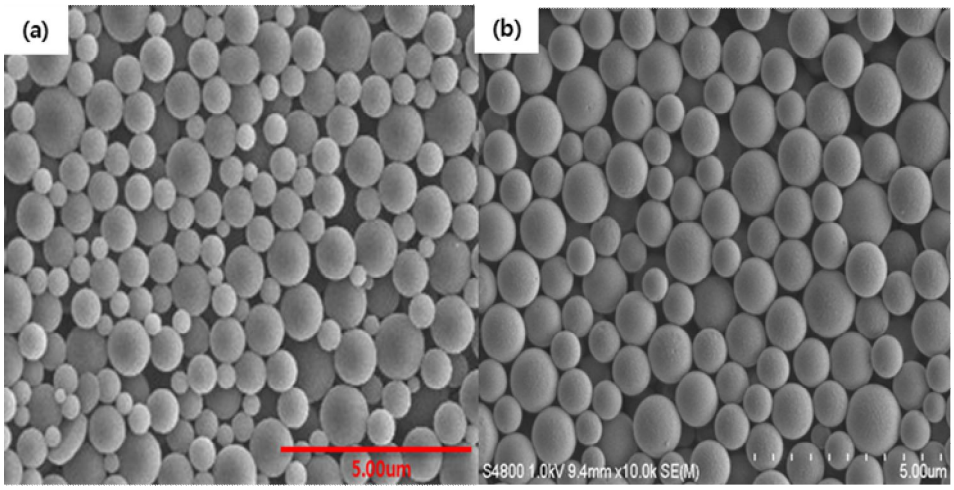

Figure 9. SEM images of the targeted size: 1.0 µm. The magnification is 10 k, mean size for (a) is 0.79 ± 0.15 µm, and (b) is 1.00 ± 0.16 µm.

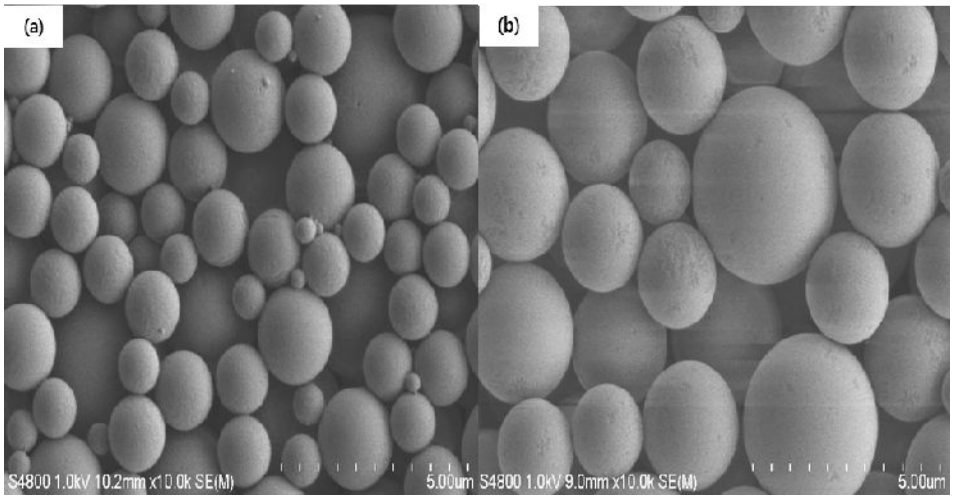

Figure 10. SEM images of the targeted size: 2.5 µm. The magnification is 10 k, mean size for (a) is 2.03 ± 0.57 µm, (b) is 2.46 ± 0.56 µm.

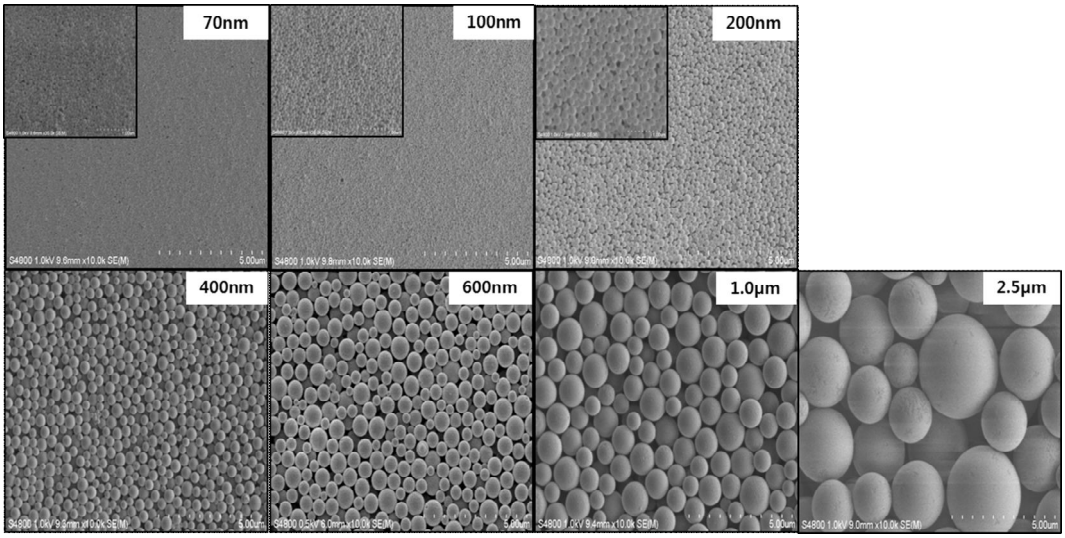

Figure 11. SEM images of the PLGA nano- and microparticles. The magnification of big size image is 10 k and small size image is 35 k. All of the particles were made in the fixed size.

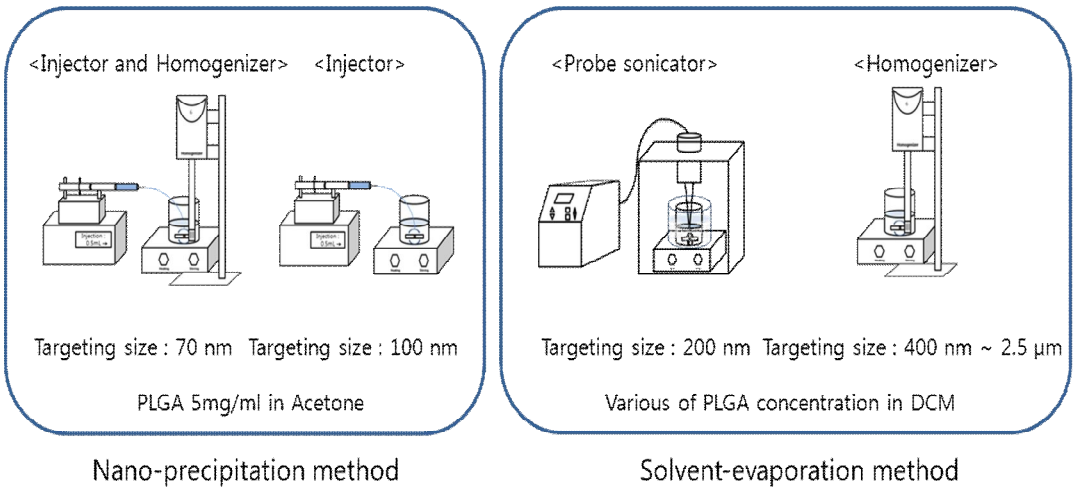

Figure 12. The method used to prepare the variety of particle size by using diverse instruments.

Chapter 3

Precisely controlled particle size of paclitaxel-loaded PLGA nano- and microparticles: Influence of particle size on drug delivery

Chapter 3

Precisely controlled particle size of paclitaxel-loaded PLGA nano- and microparticles: Influence of particle size on drug delivery

1. Introduction

Polymeric drug-loaded nanoparticles have been widely studied for targeted drug delivery. The journey of drug delivery system in the body upon administration encounters various barriers to deliver sufficient drug and targeting desire site in a controlled. PLGA (Poly (lactic-co-glycolic acid)) is approved by the US food and Drug Administration (US FDA) in various drug delivery systems in humans (1). PLGA is used as biodegradable polymers for the development of nanomedicine because its hydrolysis leads to metabolite monomers, lactic acid and glycolic acid (Figure 1). These two monomers are easily metabolized in the body. There is a minimum systemic toxicity associated with the use of PLGA for drug delivery or biomaterial applications (2, 3). PLGA is generally used for fabricating nanoparticles because of its biocompatibility and well-documented controlled drug release compared to the conventional one used to date and simplicity of administration via injection (4). The macromolecular drugs such as peptide, proteins, genes and vaccines, are successfully loaded PLGA nano-and microparticles (5).

Paclitaxel (PTX), a naturally occurring diterpenoid extracted from the bark of the Pacific Yew tree in the 1960s, is one of the best antineoplastic agents. The drug has been known to exhibit a various cancer treatments including ovarian, breast, liver, head and neck cancers (6). PTX has a poor water solubility (less than 1ug/ml) (7). Therefore, it requires co-injection in a vehicle composed of Cremophor EL and dehydrated ethanol at ratio 50:50 (v/v), causing severe side effects including hypersensitivity reaction, nephrotoxicity, neurotoxicity and cardiotoxicity

(8-13). Alternative approaches in the formulation of PTX have been suggested to remove the Cremophor EL-based vehicle and to improve the formulation of PTX such as liposomes (14, 15), micelles (16), micro- and nanoparticle (17-21) or PTX conjugated polymer (22-29). The particle size is a very important because the particles were removed by size-exclusion in the body. The need for intravenous (IV) has encouraged the size range of nanometers to a few microns (30-32). After administration, 10-30 nanoparticles are eliminated by kidney's filtering systems in renal (32, 33). 150–300 nanoparticles are found in the liver and the spleen (34) and 30–150 nanoparticles are located in bone marrow (35). Nanoparticles can escape from the circulation through the fenestrations in the endothelial barrier. Particle size impacts the extent of cellular uptake by phagocytosis and endocytosis. Particles smaller than 500 nm are usually internalized by endocytosis and particles larger than 500 nm are supposed to be internalized by phagocytosis (36). Furthermore, The solid tumor targeting effect of nanoparticles was achieved through the leaky vasculature at the tumor site and when the nanoparticles reached on the target sites and released the drug in the tumor cells. In addition, the tumor tissue is lack of the lymphatic drainage, the nanoparticles were extended retention in tumor cells. Ultimately leading to the accumulation of high concentrations of the drug at the tumor site (37, 38). Such as the enhanced permeability and retention (EPR) effect. For tumor targeting, particles less than 250 nm are preferred owing to an effective probability to the leaky endothelium (39, 40).

In the literature studying the effect of the particle size to the present; based on the; In vitro release, the smaller PLGA particle size is faster than bigger PLGA particle size (41) and the polystyrene or chitosan-modified PLGA particles known that cellular uptake is increased as the size becomes smaller (41,42). In the case of the silica (43) and silver (44) nanoparticles, the more toxicity shown as the small size of the particle. In the PLGA microparticles, drug loading is increasing as the size becomes bigger and therefore drug release rate increased with increasing particle size (45). On the other hand, DNA -encapsulating PLGA microspheres and lidocaine-loaded PLGA porous microparticles increased the release rate as the size was small (46, 47). For targeting the brain, the research result was reported that PEG was unnecessary in the small particle than 70 nm during CED (convection-enhanced delivery) (48). In gene

transfection studies, the size of 70 nanoparticle showed a 27-fold higher transfection than the size of 200 nanoparticle in COS-7 cell and a 4-fold higher transfection in HEK-293 cell (49). In the case of the gold nanoparticles, The toxicity or the cell uptake occurs in the special size. Ranging in size from 0.8 to 15 nm, the highest toxicity is in 1.4 nm (50) and ranging in size from 14 nm to 100 nm, the maximum cellular uptake by size of 50 nm (51). In this way, there was clearly the effect of the size, it did not become many researches.

Seven target sizes of the PLGA particles were established in the previous chapter. All of the particles have a narrow size distribution and precisely controlled size. The aim of this study is to investigate controlled particle size of PTX-loaded PLGA nano-and microparticles, the impact of particle size on the drug release, cellular uptake and the cytotoxicity. In the cellular uptake and the cytotoxicity of PTX-loaded nano-and microparticles were performed using cancer cells (KB).

2. Materials and Methods

2.1. Materials

Paclitaxel (PTX) was purchased from LC Laboratories (Woburn, MA, USA). PLGA copolymers (50:50 DLG 5E, i.v 0.47dL/g) was purchased from Lakeshore Biomaterials (USA). PVA (Poly vinyl alcohol, Mw 30,000~70,000, The tetrazolium dye 3-(4,5-di-methylthiazol-2-yl)-2,5-diphenyltetrazolium bromide (MTT), Dimethyl sulfoxide (DMSO), Coumarin 6 and 4′,6-Diamidino-2-phenylindole dihydrochloride (DAPI) were purchased from Sigma (USA). The fetal bovine serum (FBS), Antibiotics and Roswell Park Memorial Institute (RPMI) 1640 medium were purchased from Hycolne (USA). acetone, dichloromethane (DCM) and acetonitrile (HPLC grade) were purchased from Burdick & Jackson (USA).

2.2. Preparation of PTX-loaded PLGA nano- and microparticles

PTX-loaded PLGA nano- and microparticles were obtained by the nano- precipitation method and solvent evaporation method. The size of 70 nm and 100 nm were obtained by the nano-precipitation method and 200 nm, 400 nm, 600 nm, 1.0 μm and 2.5 μm were obtained by the solvent evaporation method.

The size of 70nm and 100 nm were obtained by the nano-precipitation technique. The size of 70 nm was simultaneous used injector with homogenizer and 100 nm was used injector. Briefly, PTX (2 mg) and PLGA (50 mg) was dissolved in 5 ml of acetone. This organic phase was injected into aqueous 1 % (w/v) PVA solution (100 ml); the emulsification was done by homogenizer (Ultra-Homogenizer IKA® Ultra-Turrax T-10 (Germany)) with a stirring rate of 20,000 rpm during 9 min in an ice bath. The resulting emulsion maintained under mechanical stirring for 18 h at 500 rpm in the Fume hood.

The size of 200 nm and 400 nm were obtained by the solvent evaporation technique. The

size of 200 nm was prepared by probe-sonicator (KFS-300N ultrasonic processor (Korea)) and 400 nm was prepared by homogenizer. Briefly, PTX (2 mg) and PLGA (50 mg) were dissolved in DCM (3 ml). This organic phase was mixed with 3 % (w/v) PVA solution (9 ml) and then the emulsification was done by probe-sonicator (100 W, 1 min) or homogenizer (30,000 rpm, 5 min) in an ice bath. The resulting emulsion was poured into an aqueous 1 % (w/v) PVA solution (20 ml) and then maintained under mechanical stirring for 3 h at 500 rpm in the Fume hood.

The size of 600 nm was obtained by the solvent evaporation technique. Briefly, PTX (2 mg) and 50 mg of PLGA were dissolved in 10 ml of DCM. This organic phase was mixed with 30 ml of aqueous 1 % (w/v) PVA solution, the emulsification was done by homogenizer (30,000 rpm, 5 min) in an ice bath. The resulting emulsion maintained under mechanical stirring for 4 h at 500 rpm in the Fume hood.

The size of 1.0 µm was obtained by the solvent evaporation technique. Briefly, PTX (4 mg) and PLGA (100 mg) were dissolved in 6 ml of DCM. This organic phase was mixed with aqueous 1 % (w/v) PVA solution (30 ml), the emulsification was done by homogenizer (30,000 rpm, 5 min) in an ice bath. The resulting emulsion maintained under mechanical stirring for 3 h at 500 rpm in the Fume hood.

The size of 2.5 µm was obtained by the solvent evaporation technique. Briefly, PTX (4 mg) and PLGA (100 mg) were dissolved in 3 ml of DCM. This organic phase was mixed with 30 ml of aqueous 1 % (w/v) PVA solution, the emulsification was done by homogenizer (20,000 rpm, 5min) in an ice bath. The resulting emulsion maintained under mechanical stirring for 3 h at 500 rpm in the Fume hood.

The size of 70 nm and 100 nm were centrifuged for 1 h at 20,000 xg (Labogene 1736R, Korea) and the particles were washed with distilled water, re-suspended and centrifuged three more to remove the residual PVA and then stored in refrigerator. The others size separation was done by various centrifuge forces.

2.3. Scanning electron microscopy (SEM)

PTX-loaded PLGA nano- and microparticles were characterized by using field emission scanning electron microscope (FE-SEM, S4800, Hitachi, Japan). The dispersed PLGA colloid in water was dropped onto a carbon tape and air dried in the hood. The carbon tape with PLGA particles was coated with platinum for 2 min under vacuum. The samples were viewed under the FE-SEM at an acceleration voltage of 1 ~ 5 kV. The particle size was measured by using ImageJ software (n=100).

2.4. Determination of paclitaxel content in the PLGA particles

Paclitaxel content in the PLGA particles was determined by HPLC (Gilson, Middleton, WI, USA). The mobile phase was a mixture of acetonitrile/ water (70:30 v/v). The reverse phase column was capcell-pak C18 (100 × 4.6 mm i.d., Pore size 5 μm). The column temperature was maintained at 30 ℃. The flow rate was set at 1.0 ml/min and the UV/VIS detection wavelength was 227 nm. Sample solution was injected at a volume of 20 μl. The HPLC was calibrated with standard solutions of 5 to 500 μg/ml of PTX dissolved in acetonitrile (correlation coefficient of R^2=0.9999). The particles were dissolved in acetonitrile. And then the tubes were centrifuged at 17.000 xg for 30 min. The supernatant was assayed by HPLC.

Encapsulation efficiency, EE (%) =Calculated drug content / Theoretical drug content
Loading efficiency, LE (%) = Weight of drug / PLGA particles weight.
Theoretical loading efficiency, TLE (%) = PLGA particles weight / Drug + polymer

2.5. In vitro drug release

PTX-loaded PLGA particles were dispersed in 1.0 ml of PBS (phosphate buffer solution, pH 7.4) containing Tween 0.1 % and incubated at 37 °C. At determined time intervals, the tubes were centrifuged at 17.000 xg for 30 min. Particles were dissolved in acetonitrile and then the

tubes were centrifuged at 17.000 xg for 30 min. Finally, the supernatant assayed by HPLC. As described in determination of paclitaxel content in the PLGA particles section.

2.6. Cell Culture

KB cells (human epidermoid cancer) were purchased from Korean Cell line Bank (Korea), RAW 264.7 cells (normal cells; macrophage) were obtained from the protein structural chemistry lab, College of Pharmacy, Pusan National University, and cultured in RPMI supplemented with 10 % (v/v) fetal bovine serum (FBS) and antibiotics (100 IU/ml of penicillin G sodium and 100 µg/ml of streptomycin sulfate). The cells were maintained in an incubator supplied with 5 % CO_2 air humidified atmosphere at 37 °C.

2.7. Evaluation of cell cytotoxicity

When the cells were confluent, then the cells were transferred to 96 well plate at a concentration of 5×10^4 cells per well. The next day, medium was replaced with a fresh one. After the cells reached around 80 %, added the paclitaxel-loaded PLGA particles of concentration (1.25 µg/ml). After 4 h, 8 h and 24 h of incubation, the medium containing particles were removed and replaced with a fresh FBS-free medium. The cells were incubated for 24 h and cytotoxicity was assayed using 3-(4,5-di-methylthiazol-2-yl)-2,5-diphenyltetrazolium bromide dye (MTT) by a microplate reader (iMark, Bio-RAD, USA).

Cell Viability (%) = (ABS (test cells) / ABS (control cells)) × 100

2.8. Cellular uptake

For confocal microscopy, KB and Raw 264.7 cells were incubated in 6-well plates at an initial density of 5×10^4 cells per well. Next day, Cells were incubated with coumarin 6 loaded PLGA particles (concentration of coumarin 6 is 0.2 µg/ml) for 2 h at 37 °C and were washed several times with cold PBS, and fixed with 4 % paraformaldehyde for 10 min. The cells were washed several times with cold PBS and incubated with 0.1 % Triton X-100 in 0.2 N NaOH for

5 min. The nucleus was stained with DAPI (2 μg/ml) for 5 min. The slides were fixed with Permount Mounting Medium (Fisher Scientific). The samples were imaged on the FV10i Fluoview confocal microscope (Olympus, Japan).

For quantitative study, cells at the initial density of 7×10^4 cells/well were plated in 12-well plates and left overnight in Raw 264.7 cells. Next day, Cells were incubated with coumarin 6 loaded PLGA particles (concentration of coumarin 6 is 0.2 μg/ml) for 1 h, 2 h and 4 h at 37 ℃. After incubation for interval times, the medium was removed and washed three times with cold PBS. Three hundred microliters of 0.1 % Triton X-100 in 0.2 N NaOH was added into each sample wells to lyse the cells. The fluorescence intensity was measured by Multimode Microplate Reader (TriStar LB 941, Berthold Technologies, Germany) with excitation wavelength at 460 nm and emission wavelength at 540 nm. PLGA particles were quantified using a BCA assay (Fisher scientific).

3. Results

3.1. Controlled particle size

The different range size of the PLGA particles was obtained by emulsion process: The size of 70 and 100 nm were produced by nano-precipitation method and 200 nm - 2.5 μm were obtained by solvent evaporation method with probe-sonicator or homogenizer. The controlled size cannot be optimized by this method. Hence, a size separation by centrifugation was done and then the size could be controlled. Precisely controlled size of PTX-loaded PLGA nano- and microparticles were fabricated. The mean size of 70 nm is (77.3 ± 13.3 nm), ~100 nm is (103.7 ± 15.9 nm), ~200 nm is (204.6 ± 26.1 nm) ~400 nm is (430.1 ± 71.5 nm), ~600 nm is (608.3 ± 116.5 nm), ~1.0 μm is (0.98 ± 0.1 μm) and ~2.5 μm is (2.45 ± 0.5 μm) (Figure 2).

3.2. In vitro drug release

Paclitaxel was released from the PTX-loaded PLGA nano- and microparticles (Figure 3). The initial fast drug release can be ascribed to particle size; while the slow and uniform release could be caused by diffusion of the large particles. In 1 h, about 47.3 ± 3.6 % of the loaded drug was released out of the size of 70 nm and 100 nm (45.9 ± 0.5 %), 200 nm (41.6 ± 1.2 %), 400 nm (23.8 ± 6.6 %), 600 nm (11.2 ± 2.3 %) 1.0μm (5.9 ± 1.9 %) and 2.5 μm (2.9 ± 2.1 %). The accumulative drug release was 70 nm (80.9 ± 3.6 %), 100 nm (71.2 ± 3.9 %), 200 nm (70.9 ± 2.1 %), 400 nm (71.0 ± 2.6 %), 600 nm (51.0 ± 2.6 %), 1.0 μm (21.2 ± 1.6 %), 2.5 μm (12.1 ± 3.9 %) in 24 h. This result proved that the size had an effect on the release. Particles with a diameter of 77 nm showed ~ 8-fold faster drug release than particles with a diameter of 2.5 μm.

3.3. Cell cytotoxicity

The cytotoxicity of paclitaxel, dmso and PTX-loaded PLGA particles were evaluated by the

MTT assay using KB cells. PTX, PTX-loaded PLGA NPs and MPs at PTX concentration of 1.25 μg/ml for 4 h, 8 h and 24 h treatment. At 4 h and 8 h, the media with particles were eliminated and then replaced with fresh media incubated for 24 h. The result for the PTX was not shown since significant cytotoxicity (Figure 4). The KB cells treated by the PTX-loaded PLGA nano-and microparticles had a higher cytotoxicity than those treated with PTX. In the case of PTX-loaded PLGA nanoparticles with concentration of 1.25 μg/ml concentration of PTX totally inhibited cell viability after 4 h of incubation while a 25.5 ~ 43.7 % decreased. The cell viability was achieved at concentrations of PTX is 1.25 μg/ml depending on the size. But the cytotoxicity did not show the other results depending on the size at 8 h and 24 h incubation. It is assumed that there is a size effect on cellular uptake until 4 h of incubation but the cellular uptake is saturated after 24 h of incubation, resulting in differential cytotoxicity. Further investigation is warranted to elucidate the effect of particle size on cellular uptake and drug activity.

3.4. Cellular uptake

Confocal microscopy of cancer cells: In KB cells, during 2 h treatment with coumarin 6-loaded PLGA nano-and microparticles (green) were closely located around the nuclei (blue, stained with DAPI), which indicated that the nanoparticles had been internalized into the cells. The size dependency was clearly seen in these images. Confocal microscopy images showed that the cells had significant uptake of 100 nm sized particles. The observed tendency of the PLGA particles distribution in KB cells was in order to 100 nm > 400 nm > 1.0 μm (Figure 5).

Confocal microscopy of macrophage: In Raw 264.7 cells, during 2 h treatment with coumarin 6-loaded PLGA nano-and microparticles. The cells were stained with DAPI (blue), and the coumarin 6-loaded nano- and microparticles are green. The cellular uptake was visualized by overlaying images obtained by FITC filter, and DAPI filter. Confocal microscopy images showed that the cells had significant uptake of 1.0 μm size particles. The tendency of the particle distribution observed in Raw 264.7 cells was in order to 1.0 μm > 400 nm > 100 nm. The larger particles showed higher uptake than smaller particles in Raw 264.7 cells (Figure

6). To detect uptake of PLGA nano- and microparticles by Raw 264.7 cells, the cellular uptake efficiency of the fluorescent coumarin 6-loaded nano- and microparticles were assayed upon 1 h, 2 h and 4 h incubation. The results showed the cellular uptake was increased as the treatment time increased. The cellular uptake was clearly dependent on the particles size; the larger particles showed higher uptake than smaller particles (Figure 7).

4. Discussion

The purpose of this study was to prepare PTX-loaded PLGA particles in seven different size ranges from 70 nm to 2.5 μm (70 nm, 100 nm, 200 nm, 400 nm, 600 nm, 1.0 μm and 2.5 μm).

All of the particles have a narrow size distribution and precisely controlled size. The size of 70 nm and 100 nm were fabricated by nano–precipitation method. In case of the particle size of 200 nm - 2.5 μm, were fabricated a similar target size and then small or large particles were completely separated by centrifugation (Table 1).

It is already published in the literature that the particle size has an effect on the drug release, as the size decreased, the drug release rate increased (52, 53). In vitro drug release study, the drug release rate was high in small size PTX-loaded PLGA particles as compare to large size particles. There was no research related to the cytotoxicity depending on the size with the drug loaded PLGA particles until present. The cytotoxicity of PTX-loaded PLGA particles clearly showed in concentration of 1.25 μg/ml. In the case of 4 h of treatment, particle size dependent cytotoxicity effect was observed. In the other 8 h and 24 h of treatment, effect was not dependent on particles size.

At 4 h treatment time, the result showed that small particles were uptake quickly and drug release was high than large-scale particles. However, when the treatment time increased, the cytotoxicity difference of the large particles and small particles was reduced and similar cytotoxicity was observed.

In cellular uptake study, the size dependent effect was prominent. The cellular uptake was increased as the size became smaller in KB cells. The size of the small particles could confirm to be effective in the cellular uptake. On the contrary, the cellular uptake was increased as the size increased in Raw 264.7 cells. As in our experiment, the literature was studied that cellular uptake increased as the size of the liposome particle increased in NR8383 cells (normal rat alveolar macrophage) (54). This result is positive. The particles in between 100 and 200 nm were used for tumor targeting. In cancer cells, cellular uptake of small size particles could be

high and the drug release effect would be increase. In Macrophage, small size particles were not nearly absorbed and the side effects would be reduced.

5. Conclusion

Precise control of particle size ranging from sub-100 nm to a few μm was achieved with paclitaxel-loaded PLGA nano-and microparticles using a combination of various methods. In vitro drug release; as a size decreased, a drug release rate increased. In cytotoxicity study; PTX-loaded particles has shown clearly dependent on the particles size for 4 h of incubation time. The smaller nanoparticle showed higher activity than larger particle. In cellular uptake, as a size decreased, cellular uptake increased in KB cells, but as a size increased, cellular uptake increased in Raw 264.7 cells. These results indicated that particle size is a crucial parameter on drug release, cellular uptake and anti-tumor activity. Therefore, particle size needs to be carefully chosen when designing particulate drug delivery systems for targeting.

6. References

1. R.A. Jain. The manufacturing techniques of various drug loaded biodegradable poly(lactide-co-glycolide) (PLGA) devices. Biomaterials. 21:2475-2490 (2000).
2. F. Danhier, E. Ansorena, J.M. Silva, R. Coco, A. Le Breton, and V. Préat. PLGA-based nanoparticles: An overview of biomedical applications. Journal of Controlled Release. 161:505-522 (2012).
3. A. Kumari, S.K. Yadav, and S.C. Yadav. Biodegradable polymeric nanoparticles based drug delivery systems. Colloids and Surfaces B: Biointerfaces. 75:1-18 (2010).
4. S. Acharyaand S.K. Sahoo. PLGA nanoparticles containing various anticancer agents and tumour delivery by EPR effect. Advanced Drug Delivery Reviews. 63:170-183 (2011).
5. R.C. Mundargi, V.R. Babu, V. Rangaswamy, P. Patel, and T.M. Aminabhavi. Nano/micro technologies for delivering macromolecular therapeutics using poly(d,l-lactide-co-glycolide) and its derivatives. Journal of Controlled Release. 125:193-209 (2008).
6. K.Y. Winand S.-S. Feng. In vitro and in vivo studies on vitamin E TPGS-emulsified poly (d, l-lactic-< i> co</i>-glycolic acid) nanoparticles for paclitaxel formulation. Biomaterials. 27:2285-2291 (2006).
7. T. Musacchio, V. Laquintana, A. Latrofa, G. Trapani, and V.P. Torchilin. PEG-PE micelles loaded with paclitaxel and surface-modified by a PBR-ligand: synergistic anticancer effect. Molecular pharmaceutics. 6:468-479 (2008).
8. R.B. Weiss, R.C. Donehower, P.H. Wiernik, T. Ohnuma, R.J. Gralla, D.L. Trump, J.R. Baker Jr, D. Van Echo, D.D. Von Hoff, and B. Leyland-Jones. Hypersensitivity reactions from taxol. Journal of Clinical Oncology. 8:1263-1268 (1990).
9. W.N. Waugh, L.A. Trissel, and V.J. Stella. Stability, compatibility, and plasticizer extraction of taxol (NSC-125973) injection diluted in infusion solutions and stored in various containers. American Journal of Hospital Pharmacy. 48:1520-1524 (1991).

10. H. Gelderblom, J. Verweij, K. Nooter, and A. Sparreboom. Cremophor EL: The drawbacks and advantages of vehicle selection for drug formulation. European Journal of Cancer. 37:1590-1598 (2001).

11. A.K. Singla, A. Garg, and D. Aggarwal. Paclitaxel and its formulations. International Journal of Pharmaceutics. 235:179-192 (2002).

12. C.M. Spencerand D. Faulds. Paclitaxel: A review of its pharmacodynamic and pharmacokinetic properties and therapeutic potential in the treatment of cancer. Drugs. 48:794-847 (1994).

13. A. Sparreboom, O. Van Tellingen, W.J. Nooijen, and J.H. Beijnen. Tissue distribution, metabolism and excretion of paclitaxel in mice. Anti-Cancer Drugs. 7:78-86 (1996).

14. A. Sharmaand R.M. Straubinger. Novel taxol formulations: Preparation and characterization of taxol-containing liposomes. Pharmaceutical Research. 11:889-896 (1994).

15. P. Crosasso, M. Ceruti, P. Brusa, S. Arpicco, F. Dosio, and L. Cattel. Preparation, characterization and properties of sterically stabilized paclitaxel-containing liposomes. Journal of Controlled Release. 63:19-30 (2000).

16. R.T. Ligginsand H.M. Burt. Polyether-polyester diblock copolymers for the preparation of paclitaxel loaded polymeric micelle formulations. Advanced Drug Delivery Reviews. 54:191-202 (2002).

17. D. Sharma, T.P. Chelvi, J. Kaur, K. Chakravorty, K. De Tapas, A. Maitra, and R. Ralhan. Novel Taxol® formulation: Polyvinylpyrrolidone nanoparticle- encapsulated Taxol® for drug delivery in cancer therapy. Oncology Research. 8:281-286 (1996).

18. S.S. Fengand G. Huang. Effects of emulsifiers on the controlled release of paclitaxel (Taxol®) from nanospheres of biodegradable polymers. Journal of Controlled Release. 71:53-69 (2001).

19. S.S. Feng, L. Mu, K.Y. Win, and G. Huang. Nanoparticles of biodegradable polymers for clinical administration of paclitaxel. Current Medicinal Chemistry. 11:413-424 (2004).

20. L. Muand S.S. Feng. Fabrication, characterization and in vitro release of paclitaxel (Taxol®) loaded poly (lactic-co-glycolic acid) microspheres prepared by spray drying technique with lipid/cholesterol emulsifiers. Journal of Controlled Release. 76:239-254 (2001).

21. G. Ruanand S.S. Feng. Preparation and characterization of poly(lactic acid)-poly(ethylene glycol)-poly(lactic acid) (PLA-PEG-PLA) microspheres for controlled release of paclitaxel. Biomaterials. 24:5037-5044 (2003).

22. Z. Xie, H. Guan, X. Chen, C. Lu, L. Chen, X. Hu, Q. Shi, and X. Jing. A novel polymer-paclitaxel conjugate based on amphiphilic triblock copolymer. Journal of Controlled Release. 117:210-216 (2007).

23. S. Biswas, N.S. Dodwadkar, P.P. Deshpande, and V.P. Torchilin. Liposomes loaded with paclitaxel and modified with novel triphenylphosphonium-PEG-PE conjugate possess low toxicity, target mitochondria and demonstrate enhanced antitumor effects in vitro and in vivo. Journal of Controlled Release. 159:393-402 (2012).

24. N. Joshi, T. Shanmugam, A. Kaviratna, and R. Banerjee. Proapoptotic lipid nanovesicles: Synergism with paclitaxel in human lung adenocarcinoma A549 cells. Journal of Controlled Release. 156:413-420 (2011).

25. P. Zhang, L. Hu, Q. Yin, Z. Zhang, L. Feng, and Y. Li. Transferrin-conjugated polyphosphoester hybrid micelle loading paclitaxel for brain-targeting delivery: Synthesis, preparation and in vivo evaluation. Journal of Controlled Release. 159:429-434 (2012).

26. A. Cirstoiu-Hapca, F. Buchegger, N. Lange, L. Bossy, R. Gurny, and F. Delie. Benefit of anti-HER2-coated paclitaxel-loaded immuno-nanoparticles in the treatment of disseminated ovarian cancer: Therapeutic efficacy and biodistribution in mice. Journal of Controlled Release. 144:324-331 (2010).

27. E. Roger, F. Lagarce, E. Garcion, and J.P. Benoit. Lipid nanocarriers improve paclitaxel transport throughout human intestinal epithelial cells by using vesicle-mediated transcytosis. Journal of Controlled Release. 140:174-181 (2009).

28. F. Danhier, N. Lecouturier, B. Vroman, C. Jérôme, J. Marchand-Brynaert, O. Feron,

and V. Préat. Paclitaxel-loaded PEGylated PLGA-based nanoparticles: In vitro and in vivo evaluation. Journal of Controlled Release. 133:11-17 (2009).

29. S.i. Sugahara, M. Kajiki, H. Kuriyama, and T.r. Kobayashi. Complete regression of xenografted human carcinomas by a paclitaxel-carboxymethyl dextran conjugate (AZ10992). Journal of Controlled Release. 117:40-50 (2007).

30. R.L. Julianoand D. Stamp. The effect of particle size and charge on the clearance rates of liposomes and liposome encapsulated drugs. Biochemical and Biophysical Research Communications. 63:651-658 (1975).

31. S.G. Muro, Carmen Champion, Julie A Leferovich, John Gajewski, Christine Schuchman, Edward H Mitragotri, Samir Muzykantov, Vladimir R. Control of Endothelial Targeting and Intracellular Delivery of Therapeutic Enzymes by Modulating the Size and Shape of ICAM-1-targeted Carriers. Mol Ther. 16: (2008).

31. L. Ilium, S.S. Davis, C.G. Wilson, N.W. Thomas, M. Frier, and J.G. Hardy. Blood clearance and organ deposition of intravenously administered colloidal particles. The effects of particle size, nature and shape. International Journal of Pharmaceutics. 12:135-146 (1982).

32. R. Nakaoka, Y. Tabata, T. Yamaoka, and Y. Ikada. Prolongation of the serum half-life period of superoxide dismutase by poly(ethylene glycol) modification. Journal of Controlled Release. 46:253-261 (1997).

33. S.M. Moghimi, A.C. Hunter, and J.C. Murray. Long-Circulating and Target-Specific Nanoparticles: Theory to Practice. Pharmacological Reviews. 53:283-318 (2001).

34. S.M. Moghimi. Mechanisms of splenic clearance of blood cells and particles: towards development of new splenotropic agents. Advanced Drug Delivery Reviews. 17:103-115 (1995).

35. S.M. Moghimi. Exploiting bone marrow microvascular structure for drug delivery and future therapies. Advanced Drug Delivery Reviews. 17:61-73 (1995).

36. J.O. Rejman, Volker Zuhorn, Inge S Hoekstra, Dick. Size-dependent internalization of particles via the pathways of clathrin- and caveolae-mediated

endocytosis. . Biochem J. 377: (2004).

37. H. Maeda. The enhanced permeability and retention (EPR) effect in tumor vasculature: the key role of tumor-selective macromolecular drug targeting. Advances in enzyme regulation. 41:189-207 (2001).

38. H. Maeda, J. Wu, T. Sawa, Y. Matsumura, and K. Hori. Tumor vascular permeability and the EPR effect in macromolecular therapeutics: a review. Journal of Controlled Release. 65:271-284 (2000).

39. M. Ferrari. Cancer nanotechnology: opportunities and challenges. Nat Rev Cancer. 5: (2005).

40. S. Nie, Y. Xing, G.J. Kim, and J.W. Simons. Nanotechnology applications in cancer. Annu Rev Biomed Eng. 9:257-288 (2007).

41. K. Yin Winand S.-S. Feng. Effects of particle size and surface coating on cellular uptake of polymeric nanoparticles for oral delivery of anticancer drugs. Biomaterials. 26:2713-2722 (2005).

42. K. Tahara, T. Sakai, H. Yamamoto, H. Takeuchi, N. Hirashima, and Y. Kawashima. Improved cellular uptake of chitosan-modified PLGA nanospheres by A549 cells. International Journal of Pharmaceutics. 382:198-204 (2009).

43. Y. Li, L. Sun, M. Jin, Z. Du, X. Liu, C. Guo, Y. Li, P. Huang, and Z. Sun. Size-dependent cytotoxicity of amorphous silica nanoparticles in human hepatoma HepG2 cells. Toxicology in Vitro. 25:1343-1352 (2011).

44. C. Carlson, S. Hussain, A. Schrand, L. K. Braydich-Stolle, K. Hess, R. Jones, and J. Schlager. Unique cellular interaction of silver nanoparticles: size-dependent generation of reactive oxygen species. The Journal of Physical Chemistry B. 112:13608-13619 (2008).

45. J. Siepmann, N. Faisant, J. Akiki, J. Richard, and J.P. Benoit. Effect of the size of biodegradable microparticles on drug release: experiment and theory. Journal of Controlled Release. 96:123-134 (2004).

46. D. Klose, F. Siepmann, K. Elkharraz, S. Krenzlin, and J. Siepmann. How porosity

and size affect the drug release mechanisms from PLGA-based microparticles. International Journal of Pharmaceutics. 314:198-206 (2006).

47. N.K. Vardeand D.W. Pack. Influence of particle size and antacid on release and stability of plasmid DNA from uniform PLGA microspheres. Journal of Controlled Release. 124:172-180 (2007).

48. J. Zhou, T.R. Patel, R.W. Sirianni, G. Strohbehn, M.-Q. Zheng, N. Duong, T. Schafbauer, A.J. Huttner, Y. Huang, and R.E. Carson. Highly penetrative, drug-loaded nanocarriers improve treatment of glioblastoma. Proceedings of the National Academy of Sciences (2013).

49. S. Prabha, W.-Z. Zhou, J. Panyam, and V. Labhasetwar. Size-dependency of nanoparticle-mediated gene transfection: studies with fractionated nanoparticles. International Journal of Pharmaceutics. 244:105-115 (2002).

50. Y. Pan, S. Neuss, A. Leifert, M. Fischler, F. Wen, U. Simon, G. Schmid, W. Brandau, and W. Jahnen-Dechent. Size-Dependent Cytotoxicity of Gold Nanoparticles. Small. 3:1941-1949 (2007).

51. B.D. Chithrani, A.A. Ghazani, and W.C. Chan. Determining the size and shape dependence of gold nanoparticle uptake into mammalian cells. Nano letters. 6:662-668 (2006).

52. C. Berkland, M. King, A. Cox, K.K. Kim, and D.W. Pack. Precise control of PLG microsphere size provides enhanced control of drug release rate. Journal of Controlled Release. 82:137-147 (2002).

53. J. Wu, T. Kong, K.W.K. Yeung, H.C. Shum, K.M.C. Cheung, L. Wang, and M.K.T. To. Fabrication and Characterization of Monodisperse PLGA-alginate Core-shell Microspheres with Monodisperse Size and Homogeneous Shells for Controlled Drug Release. Acta biomaterialia (2013).

54. S. Chono, T. Tanino, T. Seki, and K. Morimoto. Influence of particle size on drug delivery to rat alveolar macrophages following pulmonary administration of ciprofloxacin incorporated into liposomes. Journal of drug targeting. 14:557-566 (2006).

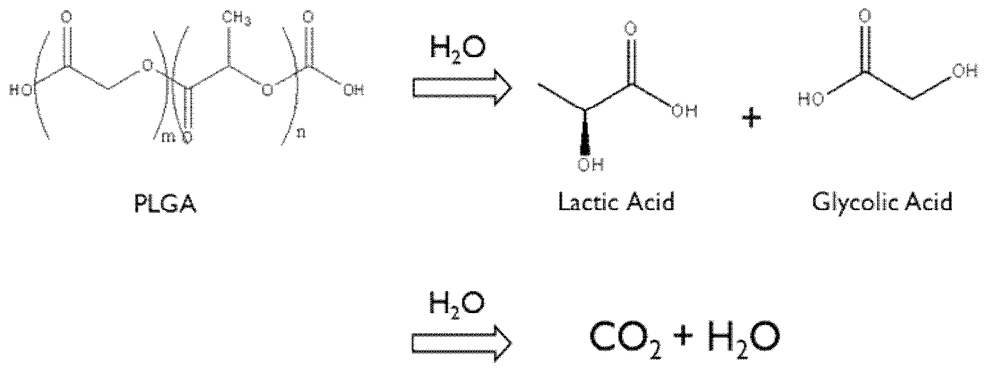

Figure 1. Hydrolysis of PLGA.

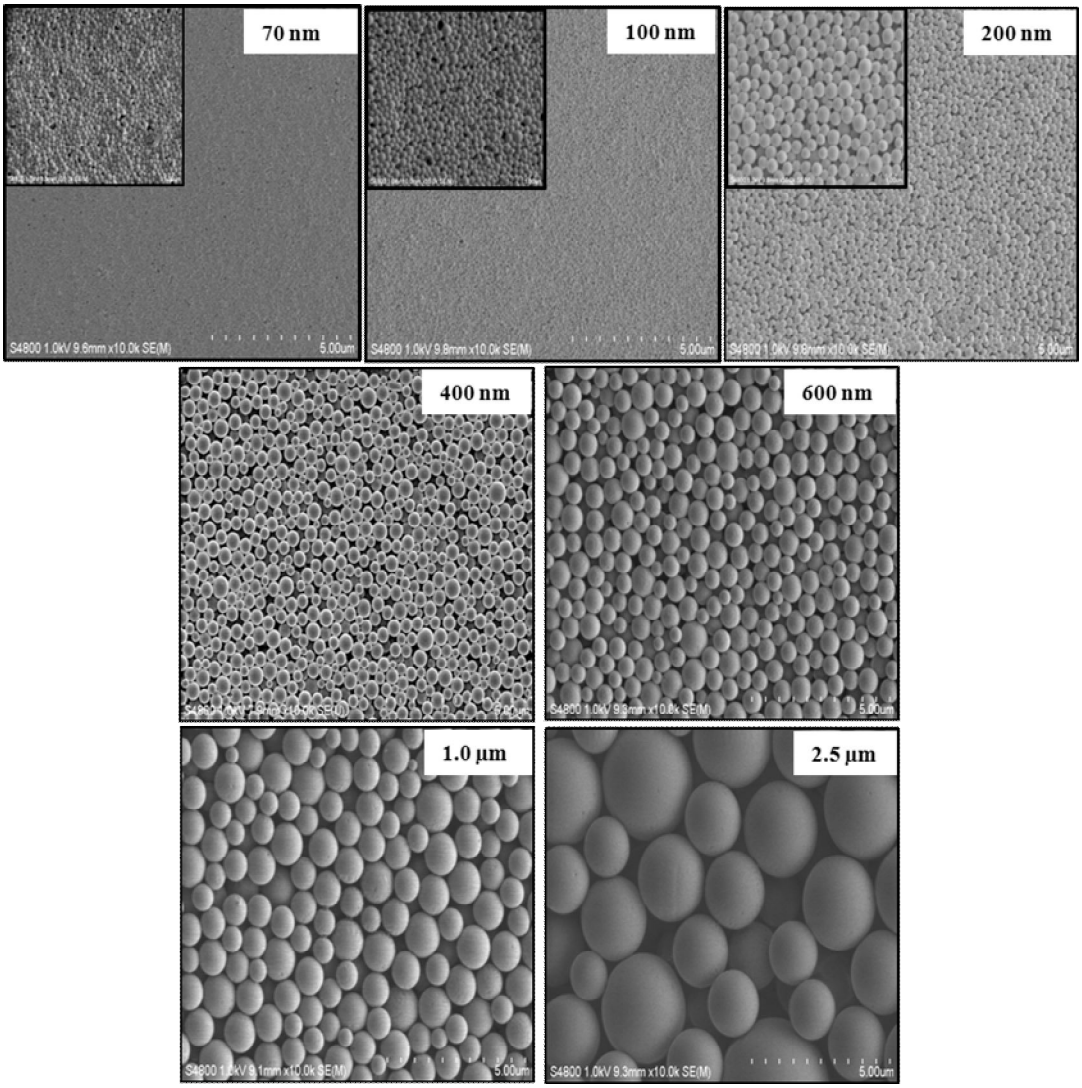

Figure 2. SEM images of the PTX-loaded PLGA nano- and microparticles. The magnification of big size image is 10 k and small size image is 35 k. All of the particles were made in the fixed size.

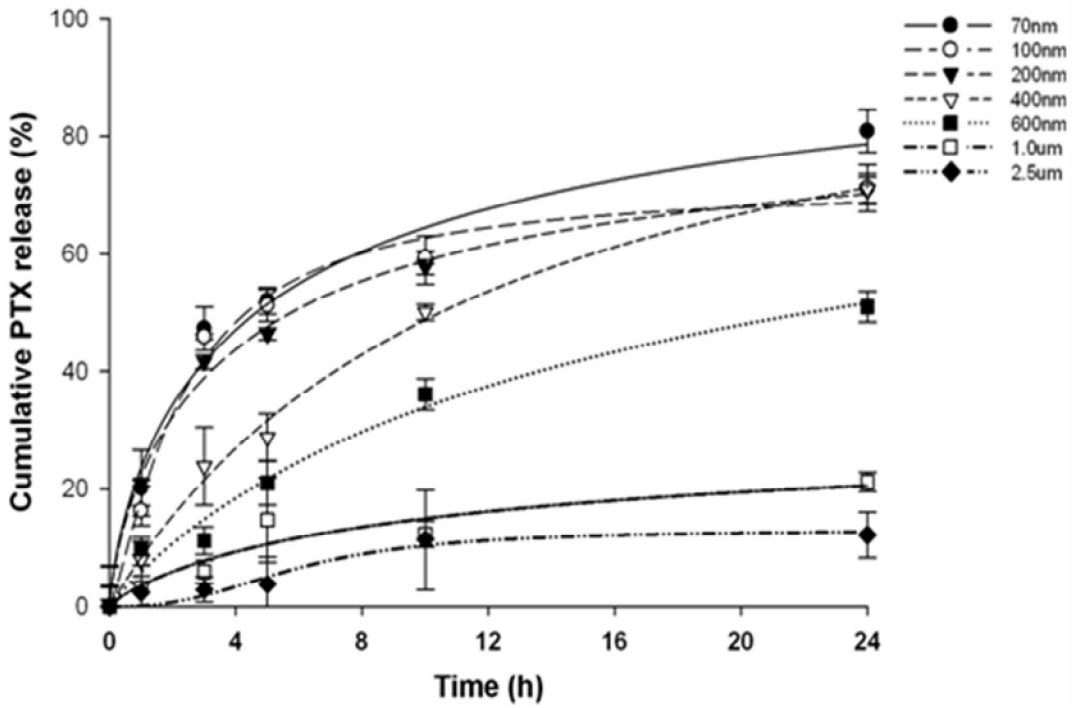

Figure 3. Cumulative release profiles of paclitaxel (PTX)-loaded PLGA nano- and microparticles. The drug-releasing increased as the size reduced.

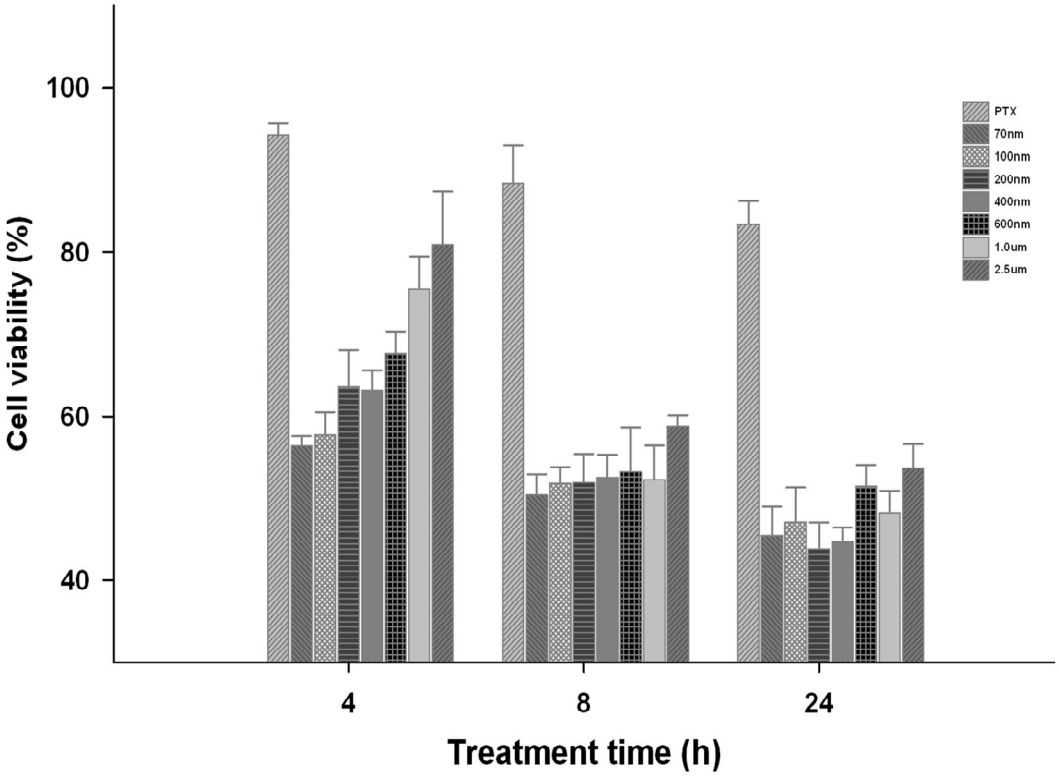

Figure 4. Cell viability of KB cells during 4 h, 8 h and 24 h treatment PTX (free drug) or PTX-loaded PLGA nano-and microparticles at the PTX concentration of 1.25 μg/ml. For 4 h of incubation, the cytotoxicity was clearly dependent on the particles size; the smaller nanoparticle showed higher activity than larger particles, indicating that the smaller particles are internalized into the cells and released the drug more efficiently than larger particles.

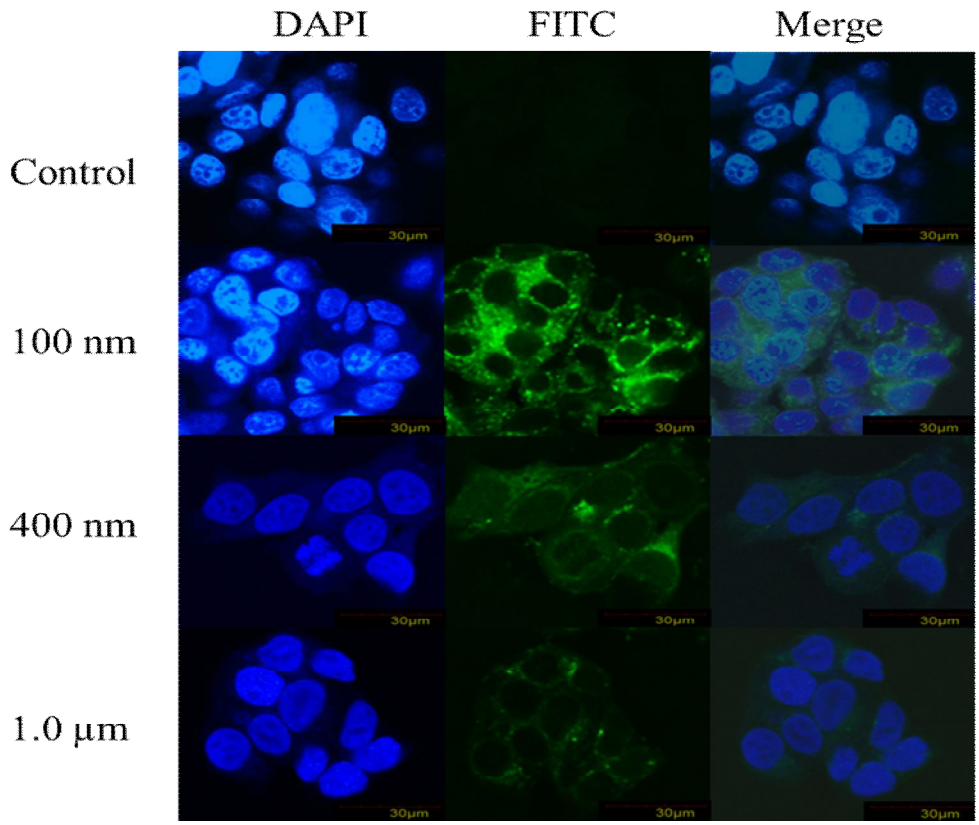

Figure 5. The PLGA nano- and microparticles uptake in KB cells during 2 h of incubation. The size dependency is clearly seen in these images. The tendency of the PLGA particle distribution observed in KB cells was in order to 100 nm > 400 nm > 1.0 µm.

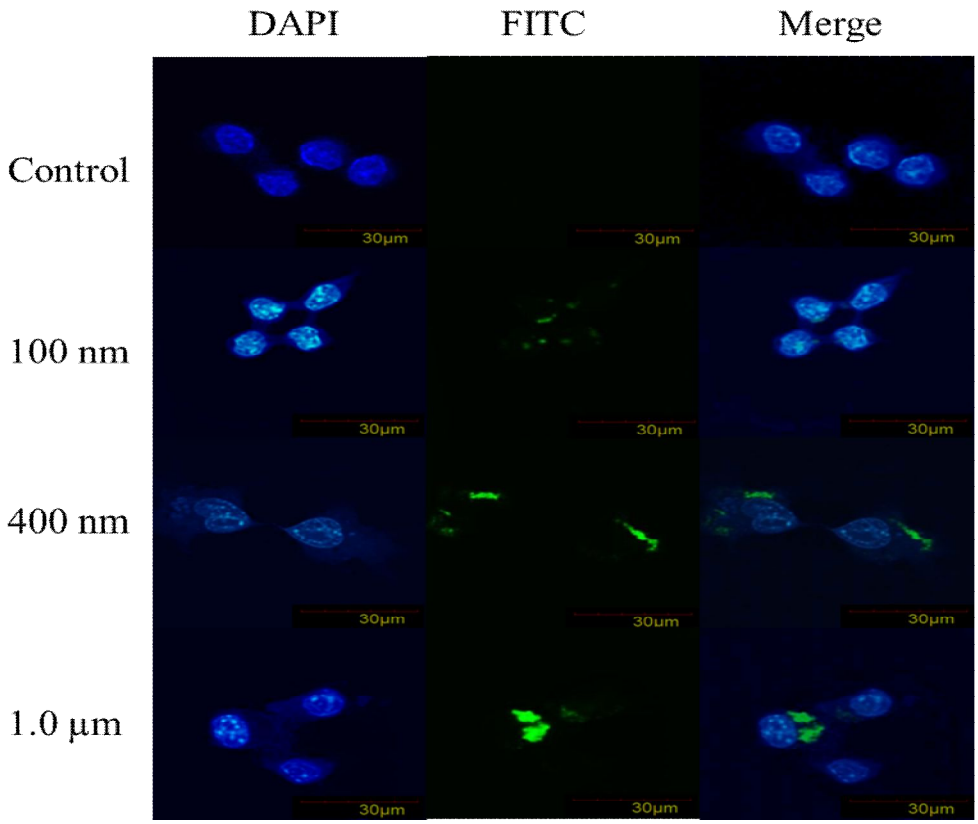

Figure 6. The PLGA nano- and microparticles uptake in Raw 264.7 cells during 2 h of incubation. Intracellular images, The scale bar is 30µm. The size dependency was clearly seen in these images. The tendency of the PLGA particle distribution observed in Raw 264.7 cells was in order to 1.0 µm > 400 nm > 100 nm. The larger particles showed higher uptake than smaller particles in Raw 264.7 cells.

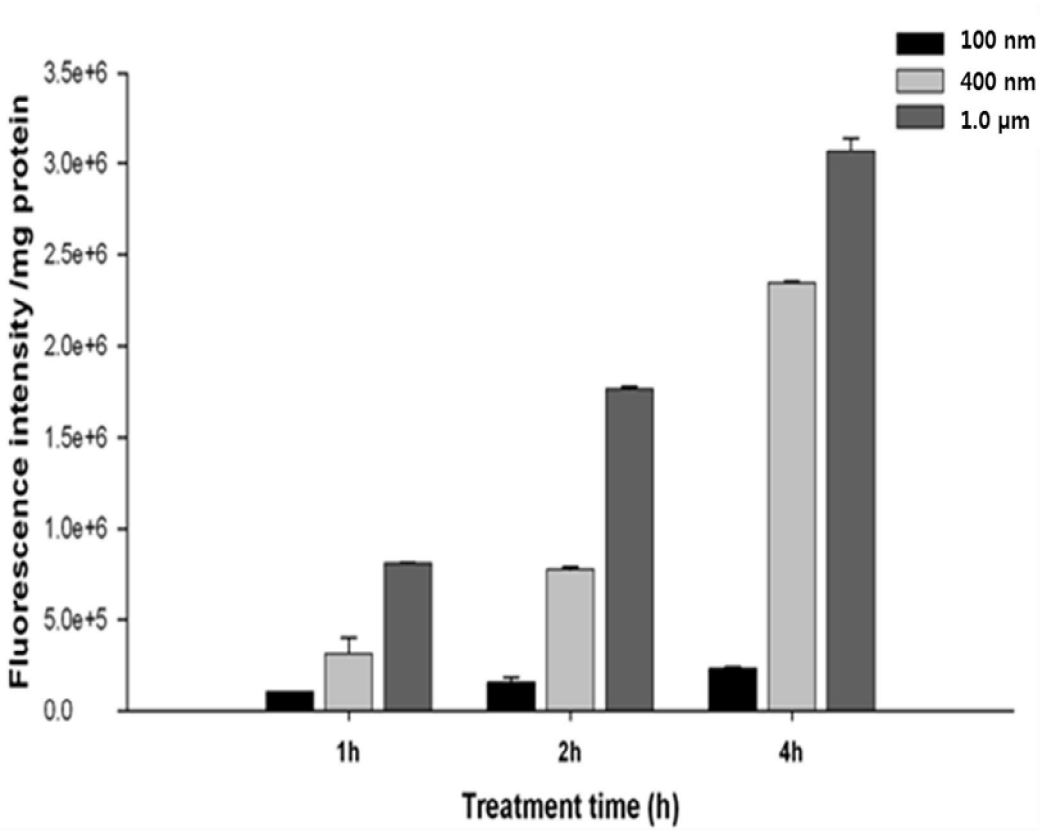

Figure 7. The PLGA nano- and microparticles uptake in Raw 264.7 cells during 1 h, 2 h and 4 h of incubation.

Chapter 4

Fabrication of surface-modifiable nonspherical PLGA particles

Chapter 4

Fabrication of surface-modifiable nonspherical PLGA particles

1. Introduction

Drug loaded polymeric particles offers several advantages over other conventional formulations. Ability of drug carriers to target sites depends on several carrier key parameters. In particular, size and surface chemistry have been extensively studied as a means to optimize carrier performance (1, 2). Recent studies, however, have shown that shape is another essential parameter of drug delivery carriers (3, 4). The role of shape in vascular dynamics has long been known in terms of its influence on the behavior of circulatory cells such as erythrocytes and platelets (5, 6). The shape of nanoparticles in the circulation is another particularly interest because it has a significant impact on hydrodynamics, and interactions with vascular targets (7, 8). For the influence of particle shape, studies have already demonstrated that nonspherical shape of particles provides and improves unique abilities that are difficult to achieve with spherical particles. This suggests that phagocytosis by macrophages is governed by the local shape of the particles and particle shape can be engineered to minimize phagocytosis (4, 9). In another study, it has been shown that rod-like particles exhibit different endocytosis properties in HeLa cells compared to the spheres depend on the parameter of particle's geometric (10).

In addition, endocytosis and intracellular distribution into cells are also affected by particle shape. Elliptical disk-shaped particles have been shown to avoid phagocytosis in a particular orientation. Based on these observations, worm-shaped particles have been engineered and shown to exhibit remarkably lower phagocytosis in comparison to spherical particles at the same volume (9, 11). Propensity of opsonized particles attach to the macrophages has also been shown to depend significantly on particle shapes (12). Since elongated particles exhibit higher contact surface area and therefore higher targeting ability compared to the spheres, they

might show a higher accumulation in the target. The elongated particles were internalized more slowly than the spherical ones (13-16). This refers to the studies showed that the elongated particles migrate slowly towards the nucleus and also oriented in a unique tangential orientation compared to the spherical particles which travel relatively faster and exhibit hexagonal packing in the cell (16, 17).

Despite a number of studies of particle shape, there has been no drug-loaded polymeric particles where surface properties are adjustable. Drug loading and surface modification is an crucial part in particle systems for drug delivery. It is the general method to make the nonspherical particles by using a Poly(vinyl alcohol) PVA film. However. Using PVA film (with hydroxyl side chains), was difficult to surface modified on PLGA particles. So, PVA film was replaced with PEMA film (with carboxylic side chains) modifying the surface on particles.

The aim of this study is to fabricate the nonspherical particles by using the PEMA (poly (ethylene-*alt*-maleic anhydride)) film to modify the surface of nonspherical particles. Using the spherical shape particles, were fabricated for preparing nonspherical particles. These particles were dispersed in an aqueous solution of polyvinyl alcohol (PVA) or Poly (ethylene-alt-maleic anhydride) (PEMA). The mixture then dried for making a film. In its simplest mode, PLGA particles were liquefied by heating above the glass transition temperature (Tg). The film formed was stretched by a film stretcher (18) (Figure .1).

2. Materials and Methods

2.1. Materials

PLGA copolymers (50:50 DLG 5E, i.v 0.47dL/g) was purchased from Lakeshore Biomaterials (Birmingham, AL, USA). paclitaxel (PTX) was purchased from LC Laboratories (Woburn, MA, USA). PVA (Poly vinyl alcohol; Mw 30,000~70,000 and PEMA (Poly (ethylene-alt-maleic anhydride); Mw 100,000~500,000 were purchased from Sigma (USA). Albumin–fluorescein isothiocyanate conjugate, N-hydroxysuccinimide (NHS) and *N*-(3-Dimethylaminopropyl)-*N*′-ethylcarbodiimide hydrochloride (EDC) were purchased from Sigma (USA). MES hydrate was purchased from Acros organic (New Jersey, USA). dichloromethane (DCM) and acetonitrile (HPLC grade) were purchased from Burdick & Jackson (Muskegon, MI, USA). Paraffin liquid and ethyl ether were purchased from Dae- jung chem (Korea).

2.2. Preparation of nonspherical particles

Poly (lactide-co-glycolide) (PLGA) nonspherical particles were prepared by the film-stretching method. Briefly, 10 % (w/v) of PVA solution was prepared in water and 2 % (w/v) glycerol was added to plasticize and reduce the glass transition temperature (Tg) of the films (9). These modifications were made consider to lowering the glass transition temperature of PLGA. Based on this method, surface modified rode shape particles were fabricated. The fabrication method of the film, initially 10 % (w/v) of PVA and 5 % (w/v) of PEMA (pH 7.8) were blended, spherical microparticles (using the surfactant; PVA or PEMA) were added to this mixture, and the films were dried on a square dish for 15 h. The film was cut into sections of 2.5 x 5 cm^2 and mounted on a custom axial made stretcher. The film was stretched in mineral oil at 58-64 °C at a rate of 0.5–1.0 $mm \cdot s^{-1}$. After stretching, the film lowered the temperature in the cold mineral oil for 5 min and washed with ethyl ether to remove residual oil. The film was then dissolved in deionized water and the stretched particles were collected by

centrifuging for 1 h at 20,000 xg, followed by washing four or five times with deionized water to remove residual PVA and PEMA.

2.2.1. Fabrication of nonspherical particles by using PVA and PEMA film

First, the size of 100 nm was fabricated using the following method: PLGA (50 mg) was dissolved in the 5 ml of DCM. This organic phase was mixed with 1 % (w/v) of PVA solution (20 ml), the mixture was sonicated by probe-sonicator (100 W, 1 min) in an ice bath. The resultant emulsion maintained under mechanical stirring for 3 h at 500 rpm in the Fume hood. The PVA and PEMA film were made as a control so that it could check whether or not the nanoparticles stretched. The 100 nm spherical particles were stretched by the film stretching method.

2.2.2. Fabrication of nonspherical particles by using the PEMA film

It has been ascertained that the carboxyl groups are more abundant on the surface of the particle if the particle and the film produced using the PEMA. Here is the method of formation of the spherical particles with the carboxylic groups on the particle surface. The nonspherical particles were prepared by film-stretching method. The particles with three different sizes were obtained by fabricating method;

100 nm: PLGA (50 mg) was dissolved in 5 ml of DCM. This organic phase was mixed with 1 % (w/v) of PVA solution (20 ml), the mixture was sonicated using a probe-sonicator (100 W, 1 min) in an ice bath. The resultant emulsion maintained under mechanical stirring for 3 h at 500 rpm in the Fume hood.

600 nm: PLGA (50 mg) was dissolved in 10 ml of DCM. This organic phase was mixed with 1 % (w/v) of PEMA solution (30 ml), the emulsification was done by homogenizer (30,000 rpm, 5 min) in an ice bath. The resultant emulsion maintained under mechanical stirring for 4 h at 500 rpm in the Fume hood.

1.0 μm: PLGA (100 mg) was dissolved in 6 ml of DCM. This organic phase was mixed with 1 % (w/v) of PEMA solution (30 ml), the emulsification was done by homogenizer (30,000

rpm, 5 min) in an ice bath. The resultant emulsion maintained under mechanical stirring for 3 h at 500 rpm in the Fume hood.

2.2.3. Effects a type of films on particle stretching

The purpose of this study is to make a film of particles using the PVA and PEMA. It is the experiment for finding out the stretching difference. Further, the surfactant used in the fabrication method of spherical particles was PVA or PEMA.

The selected particle was 600 nm. Briefly, PLGA (50 mg) was dissolved in 10 ml of DCM. This organic phase was mixed with 1 % (w/v) of PEMA solution (30 ml), the emulsification was done by homogenizer (30,000 rpm, 5 min) in an ice bath. The resultant emulsion maintained under mechanical stirring for 4 h at 500 rpm in the Fume hood.

2.2.4. Blended PVA and PEMA

In PEMA film, where the content of PEMA was 100 % and based on the idea that by mixing with PVA will change the stretching depends on the content of PEMA. Therefore PEMA blended with PVA with ratio as follows, 100/0, 82/18, 67/33, 54/46, and 43/57 %. The particles were fabricated with surfactant of PVA. Particles were used spherical particle of 1 μm size. The method was as follows; PLGA (100 mg) was dissolved in 6 ml of DCM. This organic phase was mixed with 1 % (w/v) of PVA solution (30 ml), the emulsification was done by homogenizer (30,000 rpm, 5 min) in an ice bath. The resultant emulsion maintained under mechanical stirring for 3 h at 500 rpm in the Fume hood.

2.3. Conjugation of ligands to nonspherical particles

2.3.1. Fabrication of PEMA film blended with PVA for conjugated with FITC

In PEMA film where the content of PEMA is 100 % based on the idea that by mixing with PVA will change the stretching depends on the content of PEMA. Therefore PEMA blended with PVA with ratio as follows 100/0, 54/46, 33/67, and 18/82 %. The particles were fabricated

with surfactant of PEMA or PVA. The nonspherical particles were prepared by the film-stretching method. Particles were used spherical particle of 1 μm and 2.5 μm. For PLGA particles with fluorescein, PLGA particles (20 mg) with surface conjugated were dispersed in 5 ml of MES buffer (0.1 M, pH 5.5) and then reacted with 200 μL of EDC (10 mg/ml) and 200 μl of NHS (10 mg/ml) for 2 h. Excess of unreacted EDC and NHS were removed by centrifugation 3 times with MES buffer. The activated carboxyl group of surface on particles were dispersed in 4 ml of PBS (pH 7.4) and then reacted with 200 μl of Albumin–FITC (1.0 mg/ml in PBS) for 4 h in the dark, at room temperature. Excess of unconjugated transferrin was removed by centrifuge at 3 times with PBS buffer. The samples were imaged on the FV10i Fluoview confocal microscopy (Olympus, Japan).

2.3.2. Fabrication of PVA film for conjugated with FITC

In PVA film, the particles were fabricated with surfactant of PEMA or PVA. The nonspherical particles were prepared by the film-stretching method. The particles were used spherical particle of 2.5 μm. For PLGA particles with fluorescein, PLGA particles (20 mg) with surface conjugated were dispersed in 5 ml of MES buffer (0.1 M, pH 5.5) and then reacted with 200 μL of EDC (10 mg/ml) and 200 μl of NHS (10 mg/ml) for 2 h. Excess of unreacted EDC and NHS were removed by centrifugation 3 times with MES buffer. The activated carboxyl group of surface on particles were dispersed in 4 ml of PBS (pH 7.4) and then reacted with 200 μl of Albumin–FITC (1.0 mg/mL in PBS) for 4 h– the dark, at room temperature excess of unconjugated transferrin was removed by centrifuge at 3 times with PBS buffer. The samples were imaged on the FV10i Fluoview confocal microscopy (Olympus, Japan).

2.3.3. Fabrication of FITC conjugated PLGA nanoparticles using the PEMA film blended with PVA

The object of this experiment confirms whether the surface modification of the nanoparticles is possible or not. Therefore PEMA blended with PVA with ratio as follows

100/0, 54/46, 33/67 and 0/100 %. The nanoparticles were fabricated with surfactant of PEMA. The nonspherical particles were prepared by the film-stretching method. The particles were used spherical particle of 100 nm. For PLGA particles with fluorescein, PLGA particles (20 mg) with surface conjugated were dispersed in 5 ml of MES buffer (0.1 M, pH 5.5) and then reacted with 200 μL of EDC (10 mg/ml) and 200 μl of NHS (10 mg/ml) for 2 h. Excess of unreacted EDC and NHS were removed by centrifugation 3 times with MES buffer. The activated carboxyl group of surface on particles were dispersed in 4 ml of PBS (pH 7.4) and then reacted with 200 μl of Albumin–FITC (1.0 mg/mL in PBS) for 4 h in the dark, at room temperature. Excess of unconjugated transferrin was removed by centrifuge at 3 times with PBS buffer. The samples were imaged on the FV10i Fluoview confocal microscopy (Olympus, Japan).

2.4. Scanning electron microscopy (SEM)

Nonspherical particles were characterized by using field emission scanning electron microscopy (FE-SEM, S4800, Hitachi, Japan). The dispersion of PLGA colloid in water were dropped onto a carbon tape and then dried in the fume hood and desiccator. The carbon tape with PLGA particles were coated with platinum for 2 min under vacuum. The samples were viewed under the FE-SEM at an acceleration voltage of 1 kV. The particle size was measured by using ImageJ software (n=100).

2.5. Microscopy and Confocal microscopy

For microscopy: Nonspherical particles were characterized by using microscopy (Zeiss, Axioskop, Germany). The samples were seen under the microscope lens magnification 100 x.

For Confocal microscopy: Nonspherical particles were characterized by using the FV10i Fluoview confocal microscopy (Olympus, Japan). The samples were seen under the confocal microscope lens magnification 300 x and 540 x.

3. Results

3.1. Nonspherical particles

Using PVA and PEMA film: The particles size of 100 nm was stretched with PEMA and PVA film. The nonspherical particles were made with the aspect ratio 3.1 ± 0.5 by PVA film. (b) The nonspherical particles were made with the aspect ratio 1.4 ± 0.2 by PEMA film. However, from the results obtained, the stretching particles from PEMA film only 45 % compared with the stretching particles of PVA film (Figure 2).

Using PEMA film: The three different sizes of spherical particles were fabricated with surfactant of PEMA (100 nm, 600 nm, and 1.0 μm respectively). Using the PEMA film, the particles were stretched to confirm. The obtained spherical particles (a-c), and nonspherical particles (d-f). However, the particles could be seen from the picture below number (d-f), spherical particles mixed with nonspherical particles (Figure 3).

Effects of PVA and PEMA film: After fabricating the particles size of 600 nm with surfactant of PVA or PEMA, these particles were blended with the PVA or PEMA film and examined the degree of stretching. The particles were fabricated with PVA surfactant (a) and PEMA surfactant (b). All of the particles were put into the PVA film and then stretched. The results was obtained rod-shaped particles with an aspect ratio of each is 3.5 ± 0.5 and 3.4 ± 0.5. The particles were fabricated with PVA surfactant (c) and PEMA surfactant (d). All of the particles were blended with the PEMA film and then stretched. Nonspherical particles obtained (aspect ratio; (c) 1.3 ± 0.4, (d) 1.4 ± 0.2, respectively. It could be concluded that the difference in degree of stretching depends on the composition of the film (Figure 4)

Blended PVA and PEMA: The particles were stretched by PEMA film. These particles were stretched 50 % in comparison with the PVA film. Therefore, the mixture of PVA and

PEMA was used to fabricate a film (PEMA content ranging from 43 % to 100 %). The degree of stretching depending on the content of PEMA in the film and the portion of spherical particles was increased with increasing content of PEMA. The particles were characterized by using microscopy (Zeiss, Axioskop, Germany) (Figure 5).

3.2. Determination of conjugated ligands

Effects of PVA and PEMA film: FITC-Albumin was conjugated with carboxylate group on the surface of PLGA nonspherical particles were detected by on FV10i Fluoview confocal microscopy (Olympus, Tokyo, Japan). Conjugations of the fluorescent ligand were performed for microspheres in different formulations. By using the PLGA/PEMA and PLGA/PVA were fabricated the nonspherical particles. PLGA/PVA particles have not a number of available conjugation sites. PLGA/PEMA particles showed a fluorescein at 33 %, 54 % and 100 % in PEMA blended PVA film (Figure 6), on the other hand PLGA/PVA particles only showed a fluorescein at 100 % of PEMA film (Figure 7). The degrees of stretching were depending on the content of PEMA in the film and the portion of spherical particles was increased with increased content of PEMA. The particles have a lot of air bubbles in the 54 % PEMA film, and also formed many spherical particles.

Effects of PVA film: FITC-Albumin was conjugated with carboxylate group on the surface of PLGA nonspherical particles were detected by on FV10i Fluoview confocal microscopy (Olympus, Tokyo, Japan). Conjugations of the fluorescent ligand were performed for microspheres in different formulations. By using PLGA/PEMA and PLGA/PVA, were fabricated the size of 1 μm. Both PLGA/PEMA and PLGA/PVA nonspherical particles did not show a fluorescein at 100 % PVA film (Figure 8).

Effects of PVA and PEMA film: Albumin–FITC was conjugated with carboxylate group on the surface of PLGA nonspherical particles were detected by on FV10i Fluoview confocal microscopy (Olympus, Tokyo, Japan). Conjugations of the fluorescent ligand were performed

for nanoparticles in different formulations. By using the PLGA/PEMA nanoparticles were fabricated the nonspherical particles; the nonspherical particles did not show a fluorescein at 100 % PVA film. But PLGA/PEMA particles showed a fluorescein at 33 %, 54 % and 100 % in PEMA blended PVA film. The degree of fluorescence intensity was depending on the content of PEMA in the film. Also, the degrees of stretching were depending on the content of PEMA in the film and spherical particles increased with increased content of PEMA (Figure 9).

4. Discussion

The PLGA particles were fabricated to make the nonspherical particles using film- stretching method. The method reported here is to describe how to change the spherical particles into nonspherical. The resultant shapes could be explained by the physical properties of the particles and film and the interaction between them, and generally leads to simple shapes because of few properties, primarily particle viscosity and film thickness, are relevant to the final shape. There is already initial evidence supporting the importance of shape in various scientific and technological applications, such as in the design of new carriers for drug delivery (11, 19, 20).

In the literature, nonspherical particles exhibited higher uptake compared with spherical particles (21). Accordingly the specificity of the nonspherical particles was proved. The nonspherical particles were fabricated by PVA film-stretching method. Using PVA film (with hydroxyl side chains), was difficult to surface modified on PLGA particles. So, PVA film was replaced with PEMA film (with carboxylic side chains) to modify the surface on particles. In our study, using PEMA film-stretching method, nonspherical particles were fabricated with FITC-albumin conjugated on the surface. The spherical particles were fabricated with PVA or PEMA surfactant. Then these particles were blended into the PVA film and various compositions of PEMA film, and performed conjugation with FITC-albumin on the surface of the particles after film stretching. The nonspherical particles in PVA film did not show surface fluorescence. This result presumed that the surface property of particles changed by PVA film.

PLGA/PVA particles only showed fluorescence in 100 % PEMA film. PLGA/PEMA particles showed fluorescence in over 33 % PEMA film. These results were determined that the surface of original particles has an effect in PEMA film. Also, if the particles stretched over 33 % PEMA film, it showed that the efficiency of the stretching was decreased, but the fluorescence was increased. Therefore, 33 % PEMA film was used to know that the most optimal stretching of particle.

5. Conclusion

Particles size, surface chemistry and shape are the three most important parameters in designing particle systems. Combination of the three parameter has not been applied for drug delivery because practical problems in the process of particle stretching. In this study, surface modifiable nonspherical nanoparticles made from biocompatible polymer, PLGA, loaded with anticancer drug, PTX, were successfully fabricated using new film systems. Combining size, surface chemistry and shape as well as drug loading will open a new avenue toward novel particle-based drug delivery systems.

6. References

1. S.M. Moghimi, A.C. Hunter, and J.C. Murray. Long-Circulating and Target-Specific Nanoparticles: Theory to Practice. Pharmacological Reviews. 53:283-318 (2001).

2. L. Ilium, S. Davis, C. Wilson, N. Thomas, M. Frier, and J. Hardy. Blood clearance and organ deposition of intravenously administered colloidal particles. The effects of particle size, nature and shape. International Journal of Pharmaceutics. 12:135-146 (1982).

3. G. Storm, S.O. Belliot, T. Daemen, and D.D. Lasic. Surface modification of nanoparticles to oppose uptake by the mononuclear phagocyte system. Advanced Drug Delivery Reviews. 17:31-48 (1995).

4. J.A. Championand S. Mitragotri. Role of target geometry in phagocytosis. Proceedings of the National Academy of Sciences of the United States of America. 103:4930-4934 (2006).

5. D.M. Woottonand D.N. Ku. Fluid mechanics of vascular systems, diseases, and thrombosis. Annual review of biomedical engineering. 1:299-329 (1999).

6. R.T. Schoephoerster, F. Oynes, G. Nunez, M. Kapadvanjwala, and M.K. Dewanjee. Effects of local geometry and fluid dynamics on regional platelet deposition on artificial surfaces. Arteriosclerosis, Thrombosis, and Vascular Biology. 13:1806-1813 (1993).

7. S.-Y. Lee, M. Ferrari, and P. Decuzzi. Shaping nano-/micro-particles for enhanced vascular interaction in laminar flows. Nanotechnology. 20:495101 (2009).

8. N. Doshi, B. Prabhakarpandian, A. Rea-Ramsey, K. Pant, S. Sundaram, and S. Mitragotri. Flow and adhesion of drug carriers in blood vessels depend on their shape: a study using model synthetic microvascular networks. Journal of Controlled Release. 146:196-200 (2010).

9. J.A. Championand S. Mitragotri. Shape induced inhibition of phagocytosis of polymer particles. Pharmaceutical Research. 26:244-249 (2009).

10. J. Wang, J.D. Byrne, M.E. Napier, and J.M. DeSimone. More effective nanomedicines through particle design. Small. 7:1919-1931 (2011).

11. Y. Geng, P. Dalhaimer, S. Cai, R. Tsai, M. Tewari, T. Minko, and D.E. Discher. Shape effects of filaments versus spherical particles in flow and drug delivery. Nature Nanotechnology. 2:249-255 (2007).

12. N. Doshiand S. Mitragotri. Macrophages recognize size and shape of their targets. PloS one. 5:e10051 (2010).

13. B.D. Chithrani, A.A. Ghazani, and W.C. Chan. Determining the size and shape dependence of gold nanoparticle uptake into mammalian cells. Nano letters. 6:662-668 (2006).

14. S. Muro, C. Garnacho, J.A. Champion, J. Leferovich, C. Gajewski, E.H. Schuchman, S. Mitragotri, and V.R. Muzykantov. Control of endothelial targeting and intracellular delivery of therapeutic enzymes by modulating the size and shape of ICAM-1-targeted carriers. Molecular Therapy. 16:1450-1458 (2008).

15. K. Zhang, H. Fang, Z. Chen, J.-S.A. Taylor, and K.L. Wooley. Shape effects of nanoparticles conjugated with cell-penetrating peptides (HIV Tat PTD) on CHO cell uptake. Bioconjugate chemistry. 19:1880-1887 (2008).

16. J.W. Yoo, N. Doshi, and S. Mitragotri. Endocytosis and intracellular distribution of PLGA particles in endothelial cells: effect of particle geometry. Macromolecular rapid communications. 31:142-148 (2010).

17. V.K. Kodali, W. Roos, J.P. Spatz, and J.E. Curtis. Cell-assisted assembly of colloidal crystallites. Soft Matter. 3:337-348 (2007).

18. N. Doshiand S. Mitragotri. Designer biomaterials for nanomedicine. Advanced Functional Materials. 19:3843-3854 (2009).

19. P. Decuzziand M. Ferrari. The adhesive strength of nonspherical particles mediated by specific interactions. Biomaterials. 27:5307-5314 (2006).

20. L.E. Euliss, J.A. DuPont, S. Gratton, and J. DeSimone. Imparting size, shape, and composition control of materials for nanomedicine. Chemical Society Reviews.

35:1095-1104 (2006).

21. S. Barua, J.-W. Yoo, P. Kolhar, A. Wakankar, Y.R. Gokarn, and S. Mitragotri. Particle shape enhances specificity of antibody-displaying nanoparticles. Proceedings of the National Academy of Sciences. 110:3270-3275 (2013).

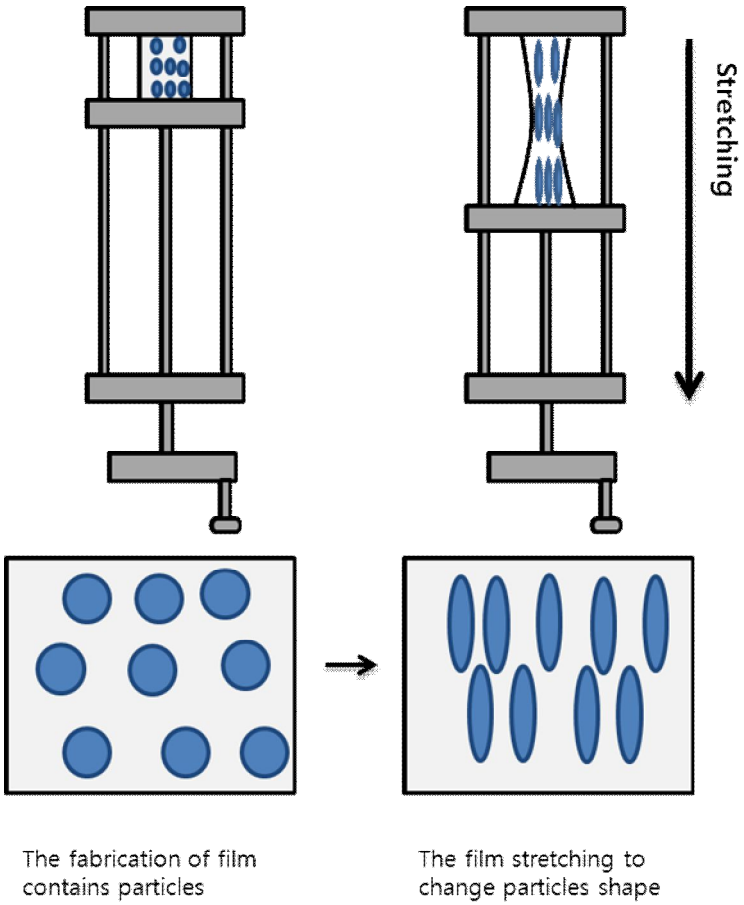

Figure 1. Fabrication methods of nonspherical particles were obtained by film stretching. The Image were reproduced from Ref. (18)

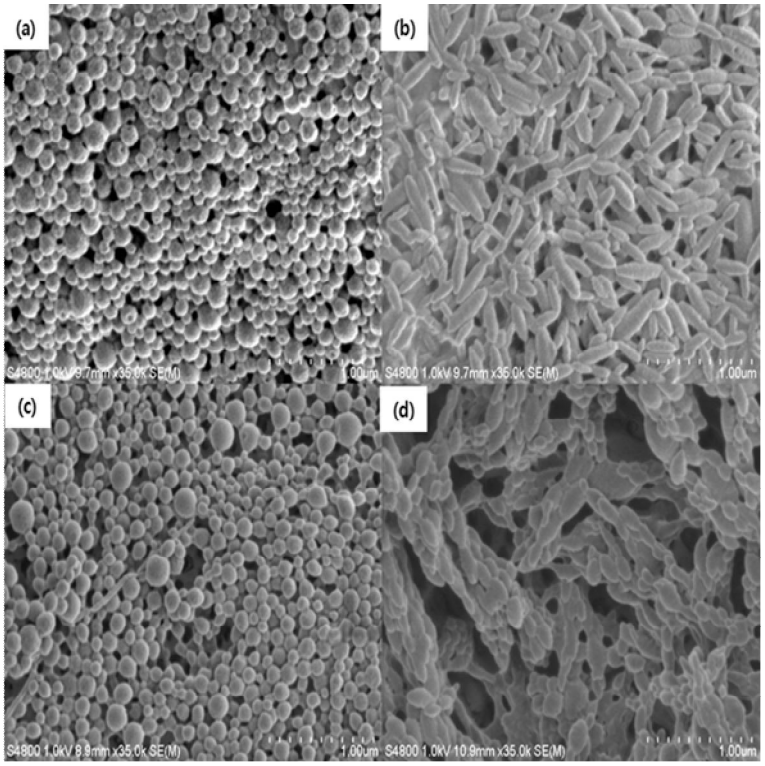

Figure 2. SEM images of spherical and nonspherical particles on the size of 100 nm. The magnification is: 35 k, PVA film; (a) size is 133.4 ± 26.4 nm and spherical particles, (b) aspect ratio is 3.1 ± 0.5 and nonspherical particles, PEMA film; (c) the mean size is 118.5 ± 24.6 nm, (d) aspect ratio is 1.4 ± 0.2 and nonspherical particles.

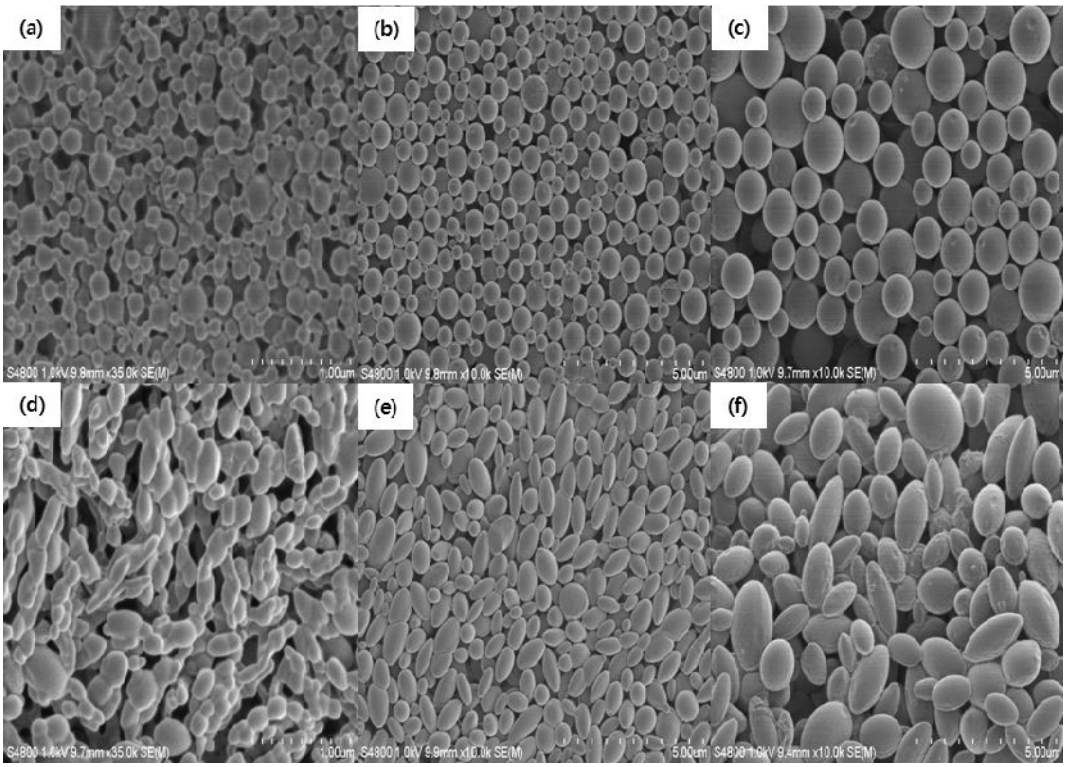

Figure 3. SEM images of spherical and nonspherical particles on different particle size. The magnification is: 10 k. The spherical particles is; (a) 100 nm, (b) 600 nm, (c) 1.0 μm. The nonspherical particles; (d) aspect ratio is 1.4 ± 0.3, (e) aspect ratio is 1.4 ± 0.2, (f) aspect ratio is 1.7 ± 0.3.

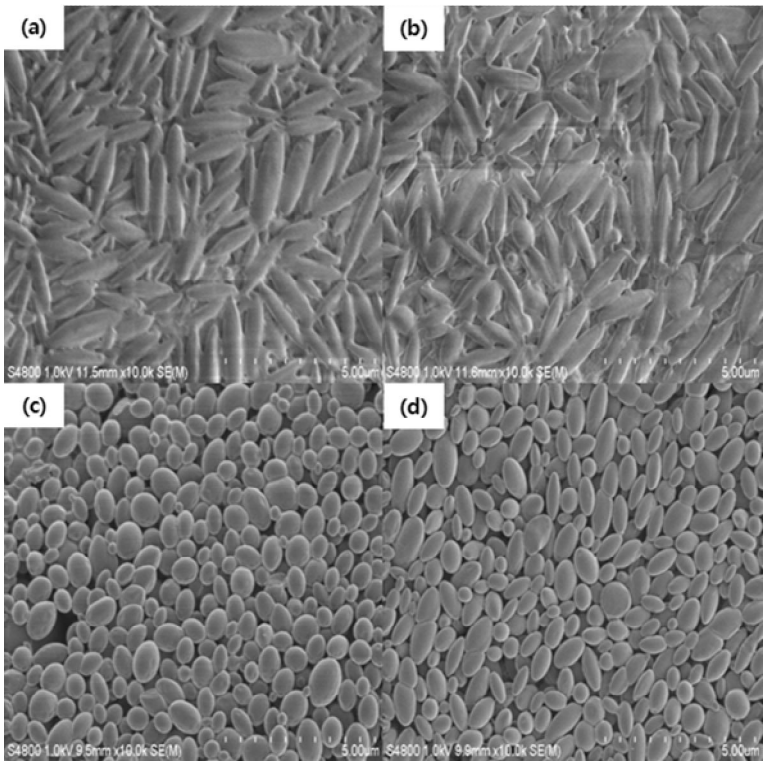

Figure 4. SEM images of spherical and nonspherical particles on the size of 600 nm. The magnification is 10 k, in PVA film; (a) is the particles fabricated by using PVA surfactant (a), aspect ratio is 3.5 ± 0.5. (b) is the particles fabricated by using PEMA surfactant and aspect ratio is 3.4 ± 0.5. In PEMA film; (c) is the particle fabricated by using PVA surfactant, aspect ratio is 1.3 ± 0.4, (d) is the particle fabricated by using PEMA surfactant, aspect ratio is 1.4 ± 0.2.

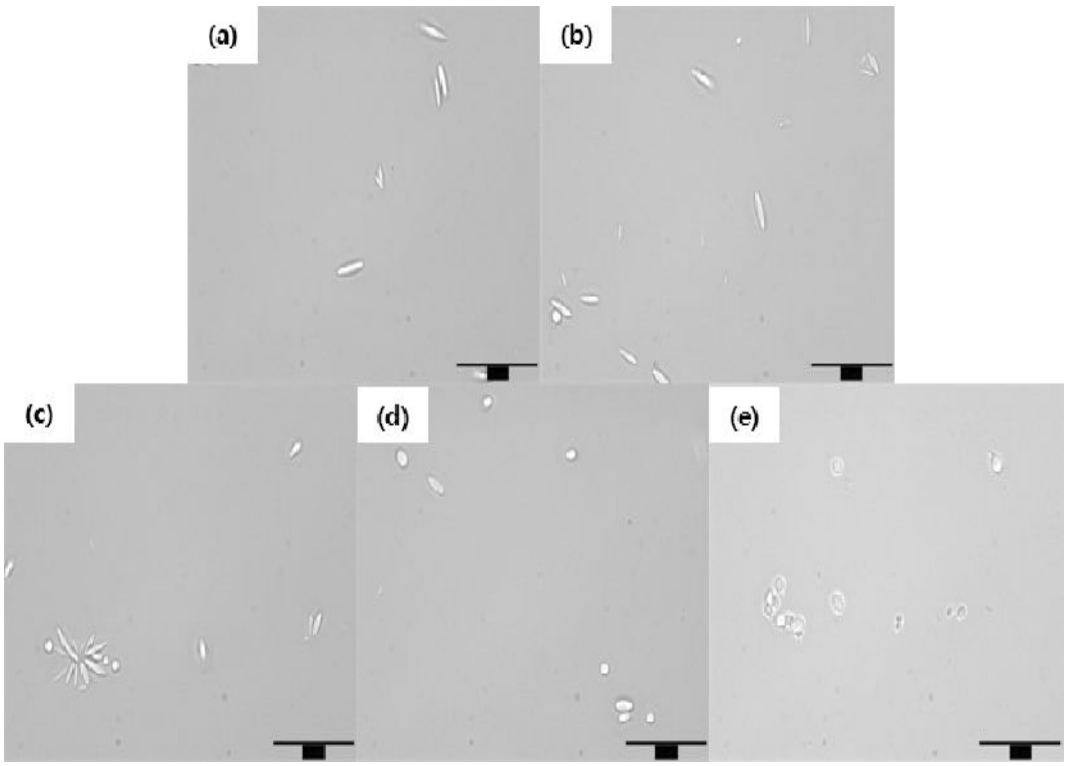

Figure 5. The microscopy images of spherical and nonspherical particles on the size of 1 µm. The magnification is 100 x and scale bar is 15 µm, All of the particles were fabricated by using PVA surfactant 1) 43 % PEMA film; aspect ratio is 3.1± 0.3, 2) 54 % PEMA film, aspect ratio is 3.0 ± 0.6, 3) 67 % PEMA film, aspect ratio is 2.7 ± 0.7, 4) 82 % PEMA film, aspect ratio is 1.6 ± 0.3. 5) 100 % PEMA film, aspect ratio is 1.5 ± 0.3.

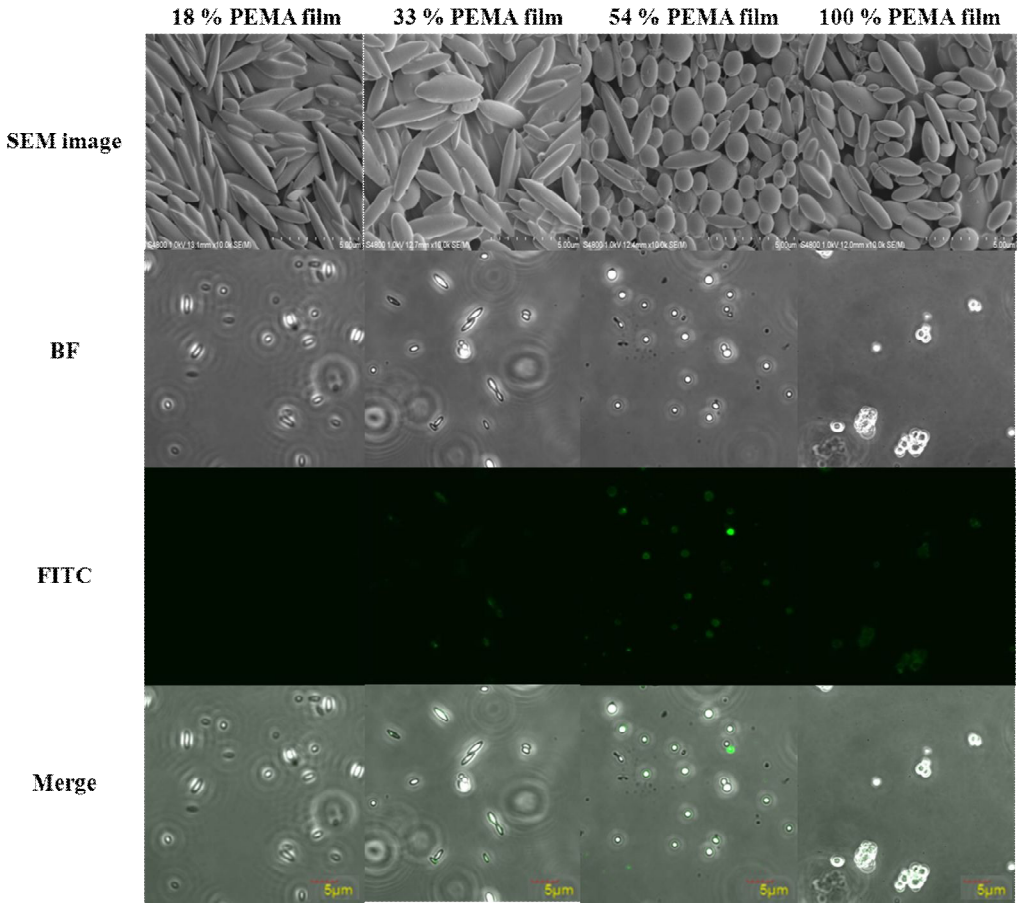

Figure 6. Comparison of capacity for coupling of Albumin-FITC to the surface of various film formulations; PLGA/PEMA microparticles, 1 µm. Scale bar, 5µm.

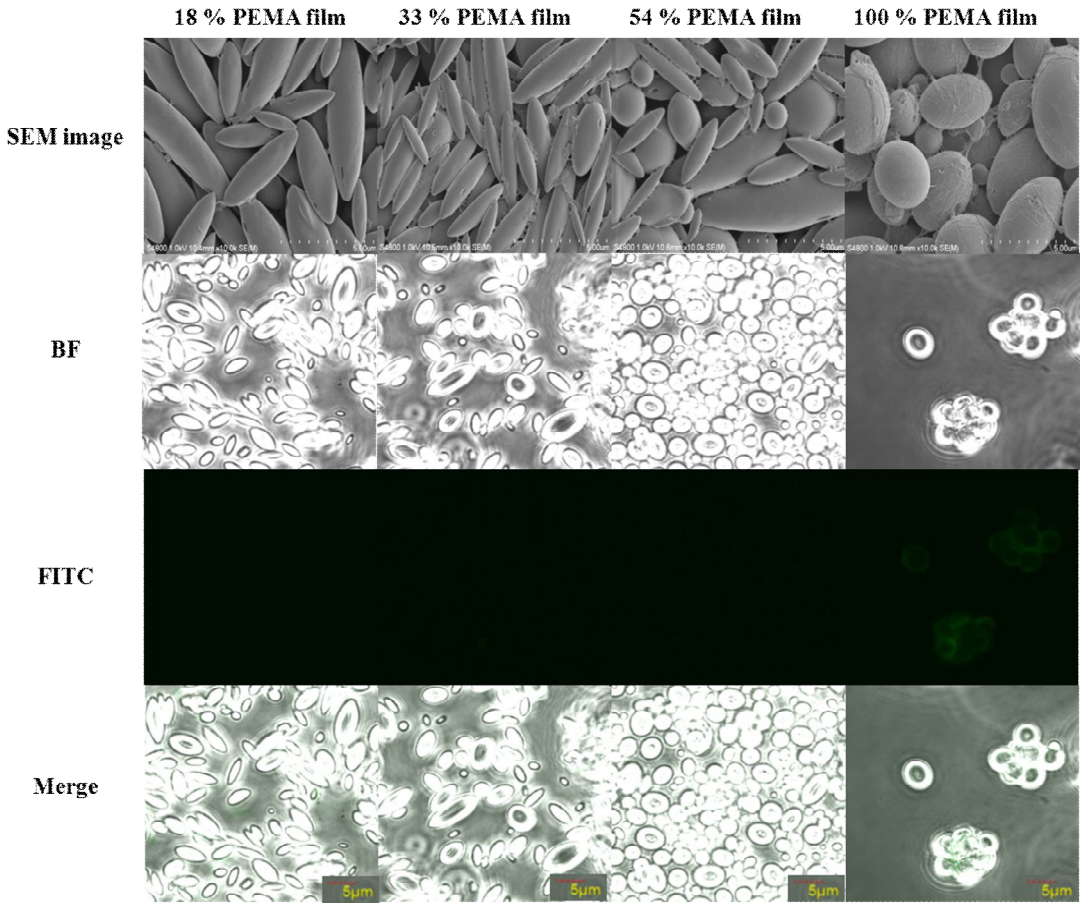

Figure 7. Comparison of capacity for coupling of Albumin-FITC to the surface of various film formulations; PLGA/PVA microparticles, 2.5 µm. Scale bar, 5 µm.

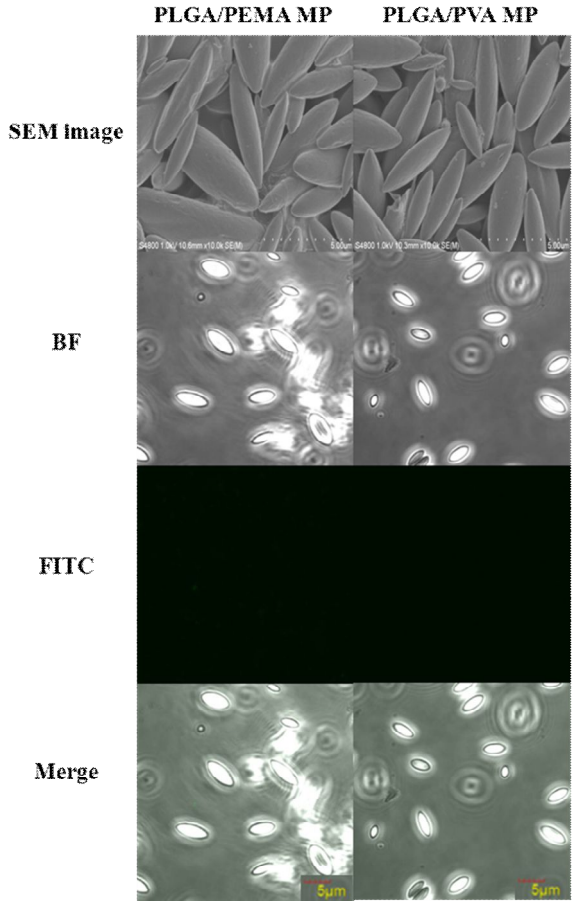

Figure 8. Comparison of capacity for coupling of Albumin-FITC to the surface of PVA film; PLGA/PEMA and PLGA/PVA microparticles, 2.5 μm. Scale bar, 5 μm.

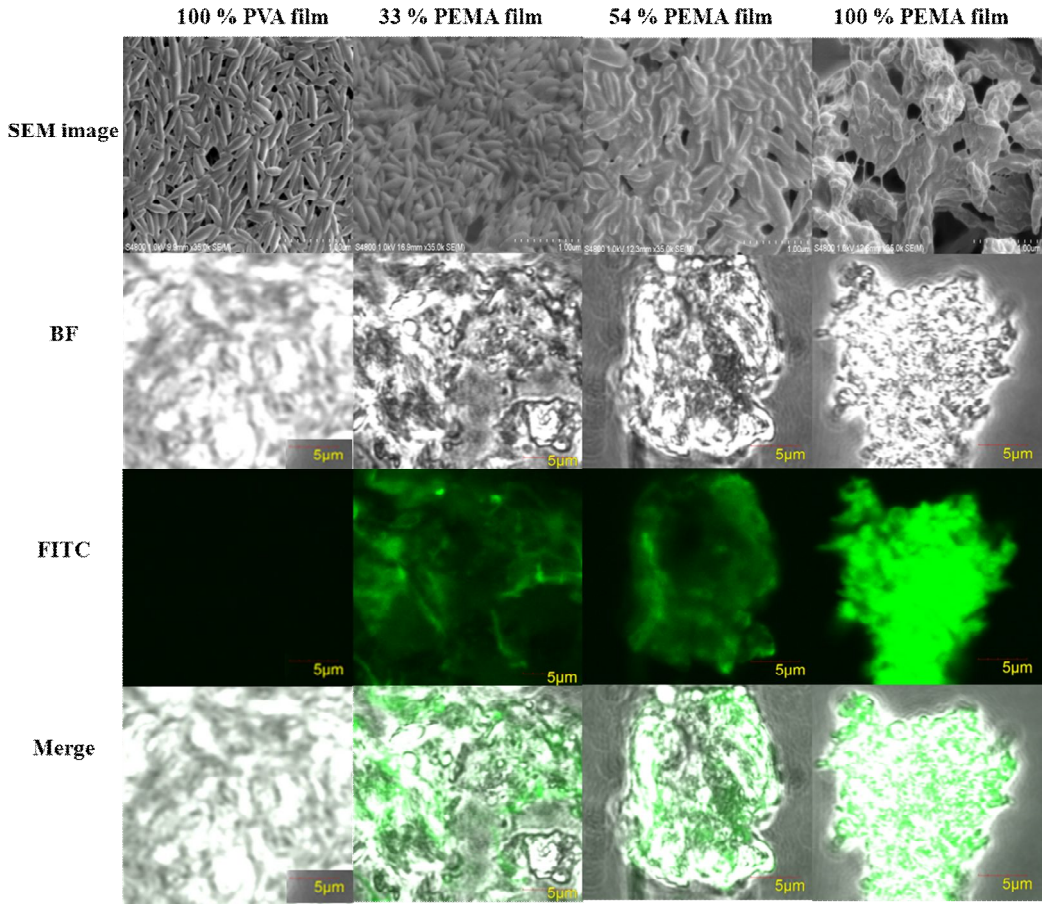

Figure 9. Comparison of capacity for coupling of Albumin-FITC to the surface of various film formulations ; 1) column is a 100 % PVA film, 2) column is a 33 % PEMA film, 3) column is a 54 % PEMA film, 4) column is a 100 % PEMA film (PLGA/PEMA nanoparticles, 100 nm). Scale bar, 5μm.

Abstract

Development of Size-, Surface Chemistry– and Shape-controlled PLGA Nanoparticles

Jin Seok Choi

Advisor: Prof. Hoo Kyun Choi, Ph.D.

Department of Food & Drug

Graduate School of Chosun University

The objective of the first study is to establish fabrication methods of precise controlled particle size of PTX-loaded PLGA nano- and microparticles. The second study was carried out to fabricate the nonspherical particles by using the PEMA (poly (ethylene-*alt*-maleic anhydride)) film to modify the surface of nonspherical particles.

The particles with various ranges of different sizes were obtained by various emulsion process. Drug release, cellular uptake and cytotoxicity studies were conducted on a variety of different particle sizes. To modify surface on PLGA particle, the film was replaced the PVA (with hydroxyl side chains) with PEMA (with carboxylate side chain). The PLGA particle was established seven different sizes (sub-100 nm, 100 nm, 200 nm, 400 nm, 600 nm, 1.0 μm and 2.5 μm). The seven sizes of PTX-loaded PLGA nano- and microparticles with a narrow size distribution were fabricated: 70 nm (77.3 ± 13.3 nm), ~100 nm (103.7 ± 15.9 nm), ~200 nm (204.6 ± 26.1 nm) ~400 nm (430.1 ± 71.5 nm), ~600 nm (608.3 ± 116.5 nm), ~1.0 μm (0.98 ± 0.1 μm) and ~2.5 μm (2.45 ± 0.5 μm), respectively. In vitro drug release, as particle size decreased drug release rate increased. In anti-tumor activity, PTX-loaded PLGA nano- and microparticles showed cytotoxicity on KB cells at the PTX concentration, whereas no cytotoxicity was observed with PTX. Cytotoxicity was confirmed to be size-dependent. In

cellular uptake, was investigated with three sizes (100 nm, 400 nm and 1.0 μm). The cellular uptake as well as the cytotoxicity was shown to be size and type of cells dependent. As particle size decreased in KB cells such as tumor cells, however the cellular uptake increased as particle size increased in Raw 264.7 cells such as macrophage.

The nonspherical particles with abundance of carboxylic group were used in conjugation with FITC-Albumin facilitated with carbodiimide as carboxyl group activator then the successful synthesis was confirmed by confocal microscopy.

In conclusion, the controlled size, surface modified and shape of the PTX-loaded PLGA particles to targeted tumor cells are expected to become major contribution in drug delivery system.

감사의 글

입학한지 엊그제 같은데 어느덧 졸업의 문턱에 서 있습니다. 학위를 취득하는 기쁨에 앞서 이 모든 것을 이룰 수 있도록 많은 도움을 주신 분들께 감사의 마음을 전합니다.

먼저 본 논문이 완성되기까지 좋은 연구 테마를 주시고 학문의 길과 방향에 대해 항상 아낌없는 지도와 격려로 학위의 꿈을 주신 최후균 교수님과 유진욱 교수님께 머리 숙여 감사를 드립니다. 또한 바쁘신 가운데서도 여러모로 부족한 저의 학위 논문을 교정 및 보완하여 심사하여 주신 최홍석 교수님, 기성환 교수님, 신상미 교수님께도 깊은 감사의 인사를 드립니다.

그리고 부족한 학교생활에 많은 도움이 되었던 조선대 약학대학 물리약학실험실, 약물학실험실 그리고 부산대 약학대학 약제학실험실 학생들 덕분에 무사히 박사과정을 마칠 수 있었습니다. 진심으로 감사 드립니다. 또한 식품의약학과 동기 및 선, 후배님에게도 감사의 뜻을 전합니다.

논문 쓰는 내내 항상 기도와 사랑으로 저를 지켜주시고 물심양면으로 든든한 지원군이셨던 부모님께 한없는 존경과 감사의 마음을 전하며, 형님과 형수님, 조카 승우와 다연 그리고 누님에게도 고마운 마음을 전합니다. 그리고 늘 한결 같은 마음으로 지금의 결실을 맺을 수 있도록 큰 사랑으로 저를 믿어주신 장인, 장모님 그리고 처남에게 말로 다 할 수 없는 감사를 드리며 자랑스러운 사위로 살아갈 것을 약속 드립니다.

마지막으로, 힘든 학업 중에서도 직장일, 가정일 무엇이든지 힘든 내색 하지 않고 묵묵히 도와준 아내에게 무한한 감사와 태어난 지 두 달 된 아들 지호에게 사랑한다는 말을 전하고 싶습니다. 지면을 통해서 일일이 언급하지 못하지만 그 동안 저를 아끼고 사랑해주신 모든 분들께 다시 한번 진심으로 감사 드립니다.

2013년 12월 최진석 올림

저작물 이용 허락서

학과	식품의약학과	학번	20107465	과정	박사
성명	한글: 최 진석 한문: 崔 津 碩 영문: Choi Jin Seok				
주소	광주광역시 동구 산수동 542-23 번지				
연락처	E-mail : c34281@gmail.com				
논문제목	한글 : 입자크기, 입자표면수식 및 입자모양이 조절된 PLGA 나노입자의 개발				
	영문 : Development of Size-, Surface Chemistry-and Shape-controlled PLGA Nanoparticles				

본인이 저작한 위의 저작물에 대하여 다음과 같은 조건 아래 조선대학교가 저작물을 이용할 수 있도록 허락하고 동의합니다.

- 다 음 -

1. 저작물의 DB 구축 및 인터넷을 포함한 정보통신망에의 공개를 위한 저작물의 복제, 기억장치에의 저장, 전송 등을 허락함.
2. 위의 목적을 위하여 필요한 범위 내에서의 편집과 형식상의 변경을 허락함. 다만, 저작물의 내용변경은 금지함.
3. 배포·전송된 저작물의 영리적 목적을 위한 복제, 저장, 전송 등은 금지함.
4. 저작물에 대한 이용기간은 5 년으로 하고, 기간종료 3 개월 이내에 별도 의사 표시가 없을 경우에는 저작물의 이용기간을 계속 연장함.
5. 해당 저작물의 저작권을 타인에게 양도하거나 출판을 허락을 하였을 경우에는 1 개월 이내에 대학에 이를 통보함.
6. 조선대학교는 저작물 이용의 허락 이후 해당 저작물로 인하여 발생하는 타인에 의한 권리 침해에 대하여 일체의 법적 책임을 지지 않음.
7. 소속 대학의 협정기관에 저작물의 제공 및 인터넷 등 정보통신망을 이용한 저작물의 전송·출력을 허락함.

동의 여부 : 동의(○) 반대 ( )

2014 년 1 월

저작자 : 최진석 (인)

조선대학교 총장 귀하